hep-ph/0701229
CERN-PH-TH/2007-003
UMN–TH–2536/07
FTPI–MINN–07/03

On the Feasibility of a Stop NLSP in Gravitino Dark Matter Scenarios

J. L. Diaz-Cruz[1*], **John Ellis**[2], **Keith A. Olive**[3] and **Yudi Santoso**[4]

[1] *Facultad de Ciencias Físico-Matemáticas, BUAP*
Apdo. Postal 1364, C.P.72000 Puebla, Pue, México
[2] *TH Division, CERN, Geneva, Switzerland*
[3] *William I. Fine Theoretical Physics Institute,*
University of Minnesota, Minneapolis, MN 55455, USA
[4] *Department of Physics and Astronomy, University of Victoria,*
Victoria, BC, V8P 1A1, Canada

Abstract

We analyze the possibility that the lighter stop $\tilde{t}_1$ could be the next-to-lightest supersymmetric particle (NLSP) in models where the gravitino is the lightest supersymmetric particle (LSP). We do not find any possibility for a stop NLSP in the constrained MSSM with universal input soft supersymmetry-breaking masses at the GUT scale (CMSSM), but do find small allowed regions in models with non-universal Higgs masses (NUHM). We discuss the cosmological evolution of stop hadrons. Most $\tilde{t}_1 qq$ 'sbaryons' and the corresponding 'antisbaryons' annihilate with conventional antibaryons and baryons into $\tilde{t}_1 \bar{q}$ 'mesinos' and the corresponding 'antimesinos', respectively, shortly after the quark-hadron transition in the early Universe, and most mesinos and antimesinos subsequently annihilate. As a result, insufficient metastable charged stop hadrons survive to alter Big Bang nucleosynthesis.

CERN-PH-TH/2007-003
January 2007

[*] On sabbatical leave at: Facultad de Ciencias, Universidad de Colima, México.

1 Introduction

In many supersymmetric models there is a multiplicatively-conserved quantum number, R parity, that guarantees the stability of the lightest supersymmetric particle (LSP). In order to avoid the LSP binding to ordinary matter, it is usually assumed to have neither strong nor electric charge [1]. Candidates for the LSP in the minimal supersymmetric extension of the Standard Model (MSSM) with gravity include sneutrinos, the lightest neutralino χ and the gravitino $\widetilde{G}$. Light sneutrinos were excluded by searches for invisible Z decays at LEP, and heavier stable sneutrinos would have been found in direct searches for the scattering of astrophysical dark matter particles on ordinary matter [2]. Thus, most attention has focused on the neutralino and the gravitino. Overlooked to some extent, a gravitino LSP is in fact quite generic even in models based on minimal supergravity (mSUGRA) [3].

In the case of a gravitino LSP [4–10], the next-to-lightest supersymmetric particle (NLSP) has a long lifetime, decaying with gravitational-strength interactions if supersymmetry breaking is mediated by supergravity. The question of the identity of the NLSP then becomes important. One generic possibility is that the NLSP is the lightest neutralino, in which case the long-lived χ would probably decay unseen, mainly via $\chi \to \widetilde{G} + \gamma$, without being stopped beforehand [4, 5]. Another generic possibility is the lightest charged slepton, probably the lighter stau $\tilde{\tau}_1$ in the MSSM with universal scalar soft supersymmetry-breaking masses (the CMSSM) [4, 6, 7, 9]. This leads to scenarios with a metastable charged sparticle that would have dramatic signatures at colliders [6, 11–14] and could affect drastically the cosmological abundances of light elements.

Electromagnetic showers from the decay products of metastable particles can alter the abundances of light elements by photo-dissociation and subsequent secondary reactions [15–17]. Moreover, hadronic showers can alter the amounts of baryons involved in the Big-Bang nucleosynthesis (BBN) processes if the lifetime $\lesssim 10^6$ s [18]. However, a more significant effect can occur in the case of a negatively-charged particle, which can form an electromagnetic bound state with a nucleus, and influence the BBN processes by lowering the Coulomb barrier for nuclear fusion [19, 20] (a catalytic effect). This has been studied within the GDM in the case of a stau NLSP in some CMSSM and mSUGRA scenarios [21].

However, there are also other possible candidates for the NLSP, such as some sneutrino [7, 22] or squark species. Among the different squark species, a generic candidate for the lightest is the lighter stop $\tilde{t}_1$ [23], which would have interesting implications for cosmology [24, 25], although there are other possibilities. In this paper we study the feasibility of scenarios with a gravitino LSP and a stop NLSP. Thus, we search for regions of the MSSM parameter

space where the $\widetilde{t}_1$ is lighter than the supersymmetric partners of all the other Standard Model particles, including the neutralino χ. A previous study showed that this is possible for large values of the soft trilinear supersymmetry-breaking parameter A_0, and the regions of the CMSSM parameter space where this happens have been delineated [25]. In traditional scenarios with conserved R parity and a heavy gravitino, these regions would have been discarded because they have a charged and coloured stable particle. However, if the gravitino $\widetilde{G}$ is the LSP and therefore constitutes the dark matter, one should explore whether some parts of these regions might survive.

There are several experimental and cosmological constraints on such a stop NLSP scenario that must be taken into account. As discussed in more detail below, the lifetime of the $\tilde{t}_1$ may be (very) long, in which case the relevant collider limits are those on (apparently) stable charged particles. We interpret the limits available from the Tevatron collider as implying that $m_{\tilde{t}_1} > 220$ GeV [26] [1]. We find no regions of the CMSSM parameter space compatible with this and other experimental constraints on $\tilde{t}_1$ NLSP scenarios. However, when we relax the CMSSM universality assumptions by considering non-universal soft supersymmetry-breaking masses for the Higgs fields (NUHM models), we do find limited regions of parameter space with a $\tilde{t}_1$ NLSP. Typical allowed values of the NUHM parameters are $m_{1/2} \sim 600$ GeV, $m_0 \sim 500$ GeV, $A_0 \sim 2100$ GeV, $\mu \sim 750$ GeV, $m_A \sim 1400$ GeV and $\tan\beta \sim 10$.

We then consider the cosmological constraints on such cases. As we show, the density of $\tilde{t}_1$ sparticles and antisparticles after cosmological freeze-out at a temperature of several GeV is strongly suppressed by strong couplings in the annihilation processes. Subsequently, at the quark-hadron transition these stops would have combined with quarks into $\tilde{t}_1 qq$ 'sbaryons' and $\tilde{t}_1 \bar{q}$ 'mesinos' and the corresponding antiparticles. The late decays of these stop hadrons could have affected the light-element abundances obtained from Big-Bang nucleosynthesis, and negatively-charged antisbaryons and antimesinos could have had dramatic bound-state effects. However, we argue that the great majority of the stop antisbaryons would have annihilated with conventional baryons to make stop antimesinos, and that most mesinos and antimesinos would subsequently have annihilated [27]. Any negatively-charged antimesinos would have decayed (relatively) rapidly into neutral mesinos. These would have been (almost) the only metastable $\tilde{t}_1$ relic particles, and would be relatively innocuous, despite their long lifetimes, because they would not have important bound-state effects. Because of the low density of $\tilde{t}_1$ after freeze-out following coannihilation and the subsequent cosmological evolution, this limited region of stop NLSP scenarios within the NUHM framework seems

[1] The LHC will probably be sensitive to a metastable $\tilde{t}_1$ that is an order of magnitude heavier.

to be viable. We conclude our paper with a brief discussion how such a scenario could be probed experimentally.

2 Stop Properties

2.1 Stop Masses, Mixing and Couplings

We start by giving some important formulae and making some crucial definitions. The (2x2) stop mass matrix may be written as:

$$\widetilde{\mathcal{M}}_{\tilde{t}}^2 = \begin{pmatrix} M_{LL}^2 & M_{LR}^2 \\ M_{LR}^{2\,\dagger} & M_{RR}^2 \end{pmatrix}, \tag{1}$$

where the entries take the forms:

$$\begin{aligned} M_{LL}^2 &= M_{\tilde{t}_L}^2 + m_t^2 + \tfrac{1}{6}\cos 2\beta\,(4m_W^2 - m_Z^2)\,, \\ M_{RR}^2 &= M_{\tilde{t}_R}^2 + m_t^2 + \tfrac{2}{3}\cos 2\beta \sin^2\theta_W\, m_Z^2\,, \\ M_{LR}^2 &= -m_t(A_t + \mu\,\cot\beta) \equiv -m_t X_t\,. \end{aligned} \tag{2}$$

The corresponding mass eigenvalues are given by:

$$m_{\tilde{t}_1}^2 = m_t^2 + \frac{1}{2}(M_{\tilde{t}_L}^2 + M_{\tilde{t}_R}^2) + \frac{1}{4}m_Z^2\cos 2\beta - \frac{\Delta}{2}, \tag{3}$$

and

$$m_{\tilde{t}_2}^2 = m_t^2 + \frac{1}{2}(M_{\tilde{t}_L}^2 + M_{\tilde{t}_R}^2) + \frac{1}{4}m_Z^2\cos 2\beta + \frac{\Delta}{2}, \tag{4}$$

where $\Delta^2 = \left(M_{\tilde{t}_L}^2 - M_{\tilde{t}_R}^2 + \frac{1}{6}\cos 2\beta(8m_W^2 - 5m_Z^2)\right)^2 + 4\,m_t^2|A_t + \mu\cot\beta|^2$. The mixing angle $\theta_{\tilde{t}}$ between the weak basis $(\tilde{t}_L, \tilde{t}_R)$ and the mass eigenstates $(\tilde{t}_1, \tilde{t}_2)$, is given by $\tan\theta_{\tilde{t}} = (m_{\tilde{t}_1}^2 - M_{LL}^2)/|M_{LR}^2|$. It is clear that obtaining a very light stop requires a very large value for the trilinear soft supersymmetry-breaking parameter [25].

The interactions of the left and right antistops $\tilde{t}_L^*$ and $\tilde{t}_R^*$ with the gravitino field $\bar{\Psi}_\mu$ and the top quark are given by [28] [2]:

$$\mathcal{L} = -\frac{1}{\sqrt{2}M}[\bar{\Psi}_\mu\gamma^\nu\gamma^\mu P_R\, t\,\partial_\nu\tilde{t}_R^* + \bar{\Psi}_\mu\gamma^\nu\gamma^\mu P_L\, t\,\partial_\nu\tilde{t}_L^*], \tag{5}$$

where the reduced Planck mass is given by $M = M_{pl}/\sqrt{8\pi}$, with $M_{pl} = 1.2\times 10^{19}$ GeV. The interaction lagrangian for $\tilde{t}_{1,2}$ is then:

$$\mathcal{L} = -\frac{1}{\sqrt{2}M}[\bar{\Psi}_\mu\gamma^\nu\gamma^\mu(\sin\theta_{\tilde{t}}P_R + \cos\theta_{\tilde{t}}P_L)\, t\,\partial_\nu\tilde{t}_1^* + \bar{\Psi}_\mu\gamma^\nu\gamma^\mu(\cos\theta_{\tilde{t}}P_R - \sin\theta_{\tilde{t}}P_L)\, t\,\partial_\nu\tilde{t}_2^*]. \tag{6}$$

[2] Note, however, that there is a typographical error in Eq.(4.31) of Ref. [28]: $(\not{p} - m_{3/2})$ should be $(\not{p} + m_{3/2})$.

The corresponding Feynman rule for the vertex is:

$$\tilde{t}_1^*(p)\bar{\Psi}^\mu\, t \to -\frac{1}{\sqrt{2}M}\,\gamma^\mu \not{p}\,(\sin\theta_{\tilde{t}}\,P_R + \cos\theta_{\tilde{t}}\,P_L). \tag{7}$$

Similarly, the Feynman rule for the chargino-gravitino-W vertex is:

$$\chi_i^-\,\bar{\Psi}^\mu W^{\nu\,-}(k) \to -\frac{m_W}{M}\gamma^\nu\gamma^\mu(A_{Li}P_R + A_{Ri}P_L) \tag{8}$$

Here $A_{Li} = U_{i2}^*\cos\beta$, and $A_{Ri} = V_{i2}^*\sin\beta$, where V and U are the matrices that diagonalize the chargino mass matrix.

2.2 Stop Decay Modes and Lifetime

There are several possible scenarios for stop decay, depending on the mass difference between the stop NLSP and the gravitino LSP $\Delta m \equiv m_{\tilde{t}_1} - m_{\widetilde{G}}$, anticipating that a stop NLSP must have $m_{\tilde{t}_1} > m_t$ from the direct search bound.

1. Case 1: $\Delta m > m_t$, i.e. small $m_{\widetilde{G}} \lesssim m_{\tilde{t}_1} - m_t$. In this case, the stop can decay directly into a top quark and a gravitino, and the rate for this dominant decay is

$$\begin{aligned}\Gamma &= \frac{1}{192\pi}\frac{1}{M_{\rm Pl}^2 m_{\widetilde{G}}^2 m_{\tilde{t}_1}^3}\left[4\left(m_{\tilde{t}_1}^2 - m_{\widetilde{G}}^2 - m_t^2\right) + 20\,\sin\theta_{\tilde{t}}\,\cos\theta_{\tilde{t}}\,m_t\,m_{\widetilde{G}}\right] \\ &\quad\times\left[(m_{\tilde{t}_1}^2 + m_{\widetilde{G}}^2 - m_t^2)^2 - 4m_{\tilde{t}_1}^2 m_{\widetilde{G}}^2\right]\left[(m_{\tilde{t}_1}^2 + m_t^2 - m_{\widetilde{G}}^2)^2 - 4m_{\tilde{t}_1}^2 m_t^2\right]^{1/2}. \end{aligned}\tag{9}$$

   This decay rate is similar to that for stau decay into tau plus gravitino [4], but in this case m_t cannot be neglected. Previous results are reproduced in the limits $m_t \to 0$ and $\theta_{\tilde{t}} \to 0$.

   We show in Fig. 1 some typical numerical results for $m_{\tilde{t}_1} = 200, 300, 400$ and 500 GeV (from top to bottom), $m_{\widetilde{G}} < m_{\tilde{t}_1} - m_t$ and $m_t = 171.4$ GeV [29], for both zero stop mixing (red solid line) and maximal mixing (blue dashed line) We see that the stop lifetime is relatively insensitive to the stop mixing angle $\theta_{\tilde{t}}$ [3], but depends sensitively on the sparticle masses, and ranges between 10^3 and 10^9 s. Clearly, this is extremely long compared with the QCD hadronization time-scale, so that the stop NLSP (unlike the t quark) forms metastable hadrons, whose spectroscopy and phenomenology we consider below. Moreover, this lifetime range is also very long on the typical time-scales of collider experiments, which must therefore consider how to search for these stop hadrons. Indeed, the stop lifetime fits into the range where the cosmological effects considered in [16, 18, 19, 21] become important.

[3] Typical values in the allowed stop NLSP region in the NUHM are $\theta_{\tilde{t}} \sim 1.3$.

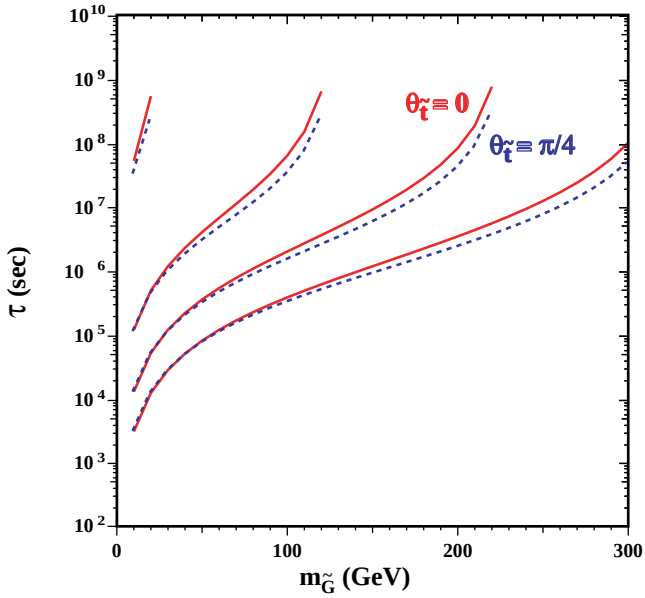

Figure 1: *The stop lifetime as a function of* $m_{\widetilde{G}}$ *for* $m_{\tilde{t}_1} = 200, 300, 400$ *and* 500 *GeV (top to bottom), shown for the case of the two-body decay* $\tilde{t}_1 \to \widetilde{G}t$*, the dominant mode for* $m_{\widetilde{G}} < m_{\tilde{t}_1} - m_t$*, assuming zero stop mixing (red solid line) and maximal mixing (blue dashed line).*

2. Case 2: $m_W + m_b < \Delta m < m_t$. In this case, the dominant decays are into the three-body final state $\widetilde{t}_1 \to \tilde{G} + W + b$. We identify three tree-level decay diagrams, proceeding via t, $\tilde{b}$ and chargino exchange. The amplitudes are

$$\mathcal{M}_t = C_t P_t(q_1) \bar{\Psi}_\mu \, p^\mu [A_{\tilde{t}} + B_{\tilde{t}} \gamma_5] (\not{q}_1 + m_t) \gamma^\rho \epsilon_\rho(k) P_L \, v(p_2), \tag{10}$$

$$\mathcal{M}_{\tilde{b}_i} = C_{\tilde{b}_i} P_{\tilde{b}_i}(q_2) \bar{\Psi}_\mu \, q_2^\mu [a_i P_L + b_i P_R] \, p^\rho \epsilon_\rho(k) \, v(p_2), \tag{11}$$

$$\mathcal{M}_{\chi_i^+} = C_{\chi^+} P_{\chi_i^+}(q_3) \bar{\Psi}_\mu \gamma^\rho \epsilon_\rho(k) \gamma^\mu [V_i + A_i \gamma_5] (\not{q}_3 + m_\chi) [S_i + P_i \gamma_5] v(p_2), \tag{12}$$

where $C_t = g_2/2M$, $C_{\tilde{b}_i} = 2 g_2 \kappa_i / M$, $C_{\chi^+} = m_W/M$, and p is the initial stop four-momentum. We define $q_1 \equiv p - p_1$, $q_2 \equiv p - k$ and $q_3 \equiv p - p_2$, with p_1, k, p_2 denoting the outgoing four-momenta of the gravitino, W boson, and b quark respectively, and $\epsilon_\rho(k)$ denotes the W polarization vector. Expressions for $A_{\tilde{t}}, B_{\tilde{t}}, a_i, b_i, \kappa_i, V_i, A_i, S_i$ and P_i are presented in the Appendix.

Squaring and summing over final polarizations we obtain:

$$|\bar{\mathcal{M}}|^2 = |\mathcal{M}_t|^2 + |\mathcal{M}_{\tilde{b}}|^2 + |\mathcal{M}_{\chi^+}|^2 + 2\,\mathrm{Re}[\mathcal{M}_t^\dagger \mathcal{M}_{\tilde{b}} + \mathcal{M}_t^\dagger \mathcal{M}_{\chi^+} + \mathcal{M}_{\tilde{b}}^\dagger \mathcal{M}_{\chi^+}]. \tag{13}$$

where the sums over sbottom and chargino indices are implicit. The individual squared

amplitudes can be written as:

$$|\mathcal{M}_{\psi_a}|^2 = C_{\psi_a}^2 \, |P_{\psi_a}(q_a)|^2 \, W_{\psi_a \psi_a}, \tag{14}$$

where $\psi_a = (t, \tilde{b}_j, \chi_k^+)$, and the functions $W_{\psi_a \psi_a}$ are functions of the scalar products of the momenta p, p_1, p_2, k. The interference terms may be written as follows:

$$\mathcal{M}_{\psi_a}^\dagger \mathcal{M}_{\psi_b} = C_{\psi_a}^* C_{\psi_b} P_{\psi_a}^*(q_a) P_{\psi_b}(q_b) W_{\psi_a \psi_b}, \tag{15}$$

where the functions $W_{\psi_a \psi_b}$ can be written also in terms of the invariants. The functions $P_{\psi_a}(q_a)$ are propagator factors, e.g., for the top quark $\psi_a = t$, and we have

$$P_t(q_1) = \frac{1}{q_1^2 - m_t^2 + i\epsilon}. \tag{16}$$

There are similar expressions for the sbottom and chargino contributions, $P_{\tilde{b}}(q_2)$ and $P_{\chi^+}(q_3)$ respectively.

Detailed formulae for the functions $W_{\psi_a \psi_a}$ and $W_{\psi_a \psi_b}$ are given in the Appendix. Using these, we calculate the decay width:

$$\frac{d\Gamma}{dx\, dy} = \frac{m_{\tilde{t}_1}^2}{256\, \pi^3} |\bar{\mathcal{M}}|^2, \tag{17}$$

where the integration limits are (in the limit when we neglect the bottom quark mass): $2\mu_G < x < 1 + \mu_G - \mu_W$ and $y_- < y < y_+$, where $\mu_i = m_i^2/m_{\tilde{t}_1}^2$ and:

$$y_\pm = \frac{1 + \mu_G + \mu_W - x}{2(1 + \mu_G - x)} [(2 - x) \pm (x - 4\mu_G)^{1/2}]. \tag{18}$$

Integrating this equation numerically, we find that in significant regions of parameter space the light stop has a lifetime of order $10^9 - 10^{14}$ s or more. Typical results are shown in Fig. 2. As expected, the typical lifetimes are orders of magnitude longer than those in Fig. 1. They are also sensitive mainly to the sparticle masses, and relatively insensitive to the stop mixing angle, as can be seen by comparing the red solid and blue dashed curves, as well as being insensitive to the sbottom mixing angle $\theta_{\tilde{b}}$, which is assumed here to vanish [4].

3. Case 3: $m_b + \Lambda_{QCD} < \Delta m < m_W + m_b$. In this case, the real W of the previous case must become virtual, and the dominant decays are four-body: $\tilde{t}_1 \to \widetilde{G} + b + \bar{q}q$ or $\ell\nu$. The decay rate for this case is further suppressed compared to Case 2, and we estimate

[4] Typical values in the allowed NUHM models discussed later are $\theta_{\tilde{b}} \sim 0.04$.

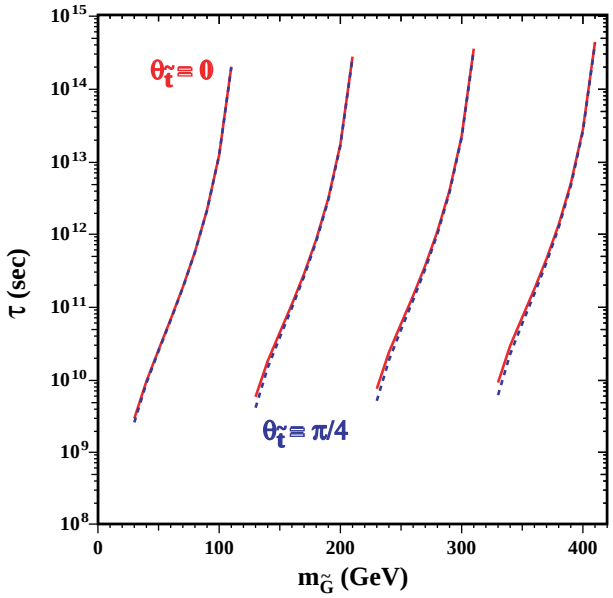

Figure 2: *The stop lifetime as a function of* $m_{\widetilde{G}}$ *for* $m_{\tilde{t}_1} = 200, 300, 400$ *and* 500 *GeV, shown for the case of three-body decays* $\tilde{t}_1 \to \widetilde{G}Wb$*, the dominant mode for* $m_W + m_b < \Delta m < m_t$*, assuming zero stop mixing (red solid line) or maximal mixing (blue dashed line).*

that the stop lifetime would in this case exceed 10^{12} s. Thus, the stop might even decay after the release of the CMB, in which case there would be important constraints from the absence of distortions in CMB spectrum. We have not explored this issue, in view of the relatively small region of parameter space concerned.

It is apparent from the above discussion that not only does the stop live long enough to hadronize and pass through collider detectors, but it may also live long enough to wreak cosmological havoc. We discuss each of these aspects in the following Sections.

3 Spectroscopy of Stop Hadrons and their Decays

The metastable stop would hadronize to produce both $\widetilde{t}_1 qq$ 'sbaryons' and $\widetilde{t}_1 \bar{q}$ 'mesinos' and their antiparticles, many of whose aspects are discussed in [30]. On general QCD principles and by analogy with the spectroscopy of charmed hadrons, one expects the $\widetilde{T}^0 \equiv \widetilde{t}_1 \bar{u}$, $\widetilde{T}^+ \equiv \widetilde{t}_1 \bar{d}$ and $\widetilde{T}_s \equiv \widetilde{t}_1 \bar{s}$ mesinos to be the lightest stop hadrons. As was pointed out in [30], one can expect the $\widetilde{T}^0$ mesino and its antiparticle to be strongly mixed. Since $m_s > m_d > m_u$, and since the $\widetilde{T}^+$ and $\widetilde{T}_s$ mesinos, being charged, would acquire additional electromagnetic mass

corrections, we expect $m_{\widetilde{T}_s} - m_{\widetilde{T}^+}$ and $m_{\widetilde{T}^+} - m_{\widetilde{T}^0}$ to be similar to the measured values of the $D_s - D^+$ and $D^+ - D^0$ mass differences, namely $\simeq 99$ MeV and $\simeq 4.8$ MeV, respectively [31].

Correspondingly, we would expect the $\widetilde{T}_s$ mesino to decay weakly into $\widetilde{T}^0 e\nu$ with a lifetime similar to that of the muon, namely $\simeq 2 \times 10^{-6}$ s, and the $\widetilde{T}^+$ mesino to decay weakly into $\widetilde{T}^0 e\nu$ with a lifetime

$$\tau_{\widetilde{T}^+} \simeq \tau_n \times \left(\frac{m_n - m_p}{m_{\widetilde{T}^+} - m_{\widetilde{T}^0}} \right)^5 \simeq 1.2 \text{ s}. \tag{19}$$

These mesino lifetimes are also such that they would pass through a typical collider detector before decaying. In the early Universe, the $\widetilde{T}_s$ would have decayed very quickly after being formed at the quark-hadron transition, whereas the $\widetilde{T}^+$, if they survive, would have decayed near the beginning of BBN, and so would not have affected its end results. Moreover, since the stable $\widetilde{T}^0$ mesino would be neutral, it could not have catalyzed light-element nucleosynthesis by bound-state effects. The only potential cosmological danger from the mesinos would be the supersymmetric decays of the $\widetilde{T}^0$ into the $\widetilde{G}$ and conventional particles, as discussed in [21], for example.

Turning now to the $\widetilde{t}_1$ sbaryons, again by analogy with the charmed baryons, we would expect the lightest state to be the $\Lambda^+_{\widetilde{T}} \equiv \tilde{t}_1 ud$, with the other sbaryons $\Sigma^{++,+,0}_{\widetilde{T}} \equiv \widetilde{t}_1 (uu, ud, dd)$, $\Xi^{+,0}_{\widetilde{T}} \equiv \widetilde{t}_1 s(u, d)$ being heavier by amounts $\sim \Lambda_{QCD}, m_s - m_{d,u}$, respectively. Just like the $\widetilde{T}_s$ mesino discussed above, these heavier sbaryons would have decayed innocuously before BBN. For example, if the $\Sigma_{\widetilde{T}} - \Lambda_{\widetilde{T}}$ mass difference were similar to the corresponding mass differences among charmed and bottom baryons, namely ~ 170 [31] to 190 MeV [32], the $\Sigma_{\widetilde{T}}$ would decay very rapidly via the strong interactions. If the $\Xi_{\widetilde{T}} - \Lambda_{\widetilde{T}}$ mass difference were similar to the corresponding mass difference among charmed baryons, namely ~ 180 MeV, the $\Xi^0_{\widetilde{T}} = \widetilde{t}_1 sd$ state would decay semileptonically with a lifetime $< 10^{-6}$ s into the $\Lambda_{\widetilde{T}}$, whereas the $\Xi^+_{\widetilde{T}} = \widetilde{t}_1 su$ state would decay semileptonically into the $\Sigma^{++}_{\widetilde{T}} = \widetilde{t}_1 uu$ with a longer lifetime $\sim 10^{-2}$ s (because of the much smaller phase space ~ 15 MeV for the decay). However, this decay would also occur by the beginning of BBN. Thus, the cosmological dangers could potentially arise only from the supersymmetric decays of the $\Lambda^+_{\widetilde{T}}$ and its antiparticle, the $\bar{\Lambda}^-_{\widetilde{T}}$, and dangerous catalysis effects could only be due to bound states of the $\bar{\Lambda}^-_{\widetilde{T}}$.

We note in passing some similarities with and differences from the case of a metastable charge -1/3 squark, such as the lighter sbottom, $\tilde{b}_1$. In this case, we would expect the lightest sbaryon to be the $\Lambda^0_{\widetilde{B}} \equiv \tilde{b}_1 ud$. Its decays might cause cosmological problems, but it could not cause dangerous bound-state effects. The nature of the lightest sbottom mesino is not so clear. The fact that the d quark is heavier than the u quark would tend to make the $\widetilde{B}^0$ mesino heavier, but the electromagnetic corrections would add to the mass

of the $\widetilde{B}^+$. Experimentally, the situation with B mesons is ambiguous, $m_{B^0} - m_{B^+} = 0.33 \pm 0.28$ MeV. However, the likelihood is probably that the $\widetilde{B}^+$ would be lighter, in which case its antiparticle, the $\widetilde{B}^-$, would generate bound-state effects, unlike the $\widetilde{T}^0$.

4 Collider Lower Limit on the Stop Mass

As we have seen, the stop would have a very long lifetime in GDM scenarios of the type considered here, and would hadronize before passing through a typical collider detector. The relative production rates of mesons and baryons containing heavy quarks are not established, and neither are the relative production rates of heavy-quark mesons containing strange quarks. We assume for simplicity that half of the produced stops hadronize into charged mesinos or sbaryons, and half into neutral stop hadrons. These would be produced embedded within hadronic jets, but conventional QCD fragmentation ideas suggest that the stop hadrons would carry essentially all the energies in these jets, with energy fractions $z_{\widetilde{T}} \sim 1 - \Lambda_{QCD}/m_{\tilde{t}_1}$.

The typical energy loss as the stop hadron passes through a detector tracking system would be very small. There would also be nuclear interactions, particularly in calorimeters. In addition to the familiar charge-exchange reactions, these would also include baryon-exchange reactions, whereby a stop mesino striking a nucleus would convert into a stop sbaryon: $\widetilde{T} + (p, n) \rightarrow (\Lambda_{\widetilde{T}}, \Sigma_{\widetilde{T}}) + n\pi$, whereas the corresponding sbaryon-to-mesino conversion would be essentially forbidden. It has been pointed out that the baryon-exchange process would be almost 100 % efficient in converting heavy mesinos to sbaryons when they traverse material with a thickness of 1 m or more [30] (see also [33]). We therefore assume for simplicity that all of the stop hadrons emerging from calorimeters into muon detectors are sbaryons, that half of them are singly-charged, and that this charge is independent of the charge of the stop hadron at production. This would imply that just a quarter of the produced stop hadrons would be singly-charged both at production and in the muon detectors. Thus, only about 1/16 of the produced stop-antistop pairs would yield a robust signature of a pair of oppositely-charged massive metastable particles.

We use here the limits set by direct searches for the pair-production of massive (meta)stable charged particles at hadron colliders to set a lower bound on the stop mass. Nunnemann [34] gives an upper limit from D0 of about 0.1 pb from a search for the pair-production of massive oppositely-charged particles, and a similar upper limit for the pair-production of stops has been presented by CDF [26], which is used to set a lower limit of 220 GeV for $m_{\tilde{t}_1}$. Gallo [35] gives a D0 upper limit on the production of neutral gluino hadrons of about 0.5 pb. Again

assuming that about a quarter of the stop hadrons are produced neutral and also appear neutral in the outer detectors, this limit gives a somewhat weaker limit on $m_{\tilde{t}_1}$. Therefore, we assume $m_{\tilde{t}_1} > 220$ GeV [26].

5 Stop NLSP in the CMSSM

We now discuss the prospects for finding a stop NLSP in the CMSSM, i.e., the simplest variant of the MSSM, in which the soft supersymmetry-breaking masses are universal at the GUT scale. Thus, we have as free parameters m_0, the universal soft scalar mass at the GUT scale, $m_{1/2}$, the universal gaugino mass at the GUT scale, A_0, the universal trilinear soft supersymmetry-breaking parameter at the GUT scale, $\tan\beta$, the ratio of the two MSSM Higgs vevs, and the sign of μ (where μ is the Higgs mixing parameter). In addition, unless we make additional assumptions, as may be motivated by supergravity models, we must consider the gravitino mass $m_{\widetilde{G}}$ as an extra free parameter, which is chosen so that the gravitino is the lightest supersymmetric particle (LSP).

We search within the CMSSM for a set of parameters where not only is the stop the NLSP, but also all the known experimental and phenomenological constraints on supersymmetry are satisfied, including the $b \to s\gamma$ decay rate [36, 37], and the LEP lower bounds on the masses of the chargino and the Higgs boson [38] [5]. In view of the ambiguity in the value of the hadronic contribution to the Standard Model value of the muon anomalous magnetic moment, $g_\mu - 2$, we omit this observable for the moment. The $B_s \to \mu^+\mu^-$ constraint is significant only for large $\tan\beta$, whereas, as we see below, the regions that are relevant to our search have relatively small $\tan\beta \sim 10$.

We choose the sign of μ to be positive, as our search indicates that negative μ has less chance of yielding a stop NLSP [6], and assume $m_t = 171.4$ GeV [29] and $m_b(m_b)^{\overline{MS}} = 4.25$ GeV. Since $m_\chi \simeq 0.43 m_{1/2}$, in order to obtain $m_\chi > m_{\tilde{t}_1} > 220$ GeV, we must set $m_{1/2} \gtrsim 520$ GeV in the CMSSM (this is relatively independent of $\tan\beta$). However, the LL and RR components of the $m_{\tilde{t}}^2$ mass matrix receive contributions of about $6m_{1/2}^2$ and $4m_{1/2}^2$ respectively, forcing one to consider large off-diagonal elements. These are of the form $m_t X_t = -m_t(A_t + \mu/\tan\beta)$, as seen in (2) [7]. Low stop mass eigenvalues therefore require a combination of high values of A_0 and relatively low values of $\tan\beta$. In fact, as we show explicitly below, only intermediate values of $\tan\beta$ have any chance of realizing

[5] We use the public Fortran code `FeynHiggs` [39] to calculate m_h.

[6] Negative μ may also be disfavoured by $b \to s\gamma$ and $g_\mu - 2$.

[7] Note that A_t signifies the value of the trilinear term at the scale $m_{\tilde{t}}$, which differs from its value A_0 at the GUT input scale.

low stop masses without upsetting the remaining phenomenological constraints. At high $\tan\beta$ the $b \to s\gamma$ constraint is not satisfied, and at low $\tan\beta$ the LEP Higgs mass bound cannot be satisfied. Our only option therefore is large A_0. Our search in the CMSSM is further complicated by the dependence of the Higgs mass on X_t. For relatively small values of $|X_t|/m_{1/2}$, the Higgs mass increases with increasing $|X_t|$. However, for $|X_t|/m_{1/2} \gtrsim 2$, the Higgs mass begins to decrease rapidly [40]. In order to obtain a light stop, we need $|X_t|/m_{1/2} \sim 6m_{1/2}/m_t$, which is too large to have any chance of satisfying the Higgs mass constraint.

In order to obtain a more comprehensive picture, we show in Fig. 3 some contour plots in $(\tan\beta, A_0)$ planes for some fixed values of m_0 and $m_{1/2}$. In panel (a) we fix $m_0 = 500$ GeV and $m_{1/2} = 400$ GeV (the gravitino mass $m_{\widetilde{G}}$ is irrelevant here). The $b \to s\gamma$ constraint, which excludes large $\tan\beta$, is shown by the green shaded region. In the allowed region, either the stop or the neutralino is the lightest sparticle in the spectrum. Above the thick purple solid line, the stop is lighter, while below it the neutralino is lighter. We also plot the $m_{\tilde{t}_1} = 220$ GeV contour, represented by the orange solid line: regions above this line have $m_{\tilde{t}_1} < 220$ GeV, and therefore are excluded. The Higgs mass constraint is represented by two red lines, the dashed line is based on a likelihood analysis, and the dot-dashed line on the face value of the Higgs mass limit, namely $m_h = 114.4$ GeV (deprecated). The constraints are satisfied only below the lines. We use the constraint determined by the likelihood function in our analysis. We see in panel (a) that there is an overlap between the stop NLSP region and the region allowed by the Higgs likelihood constraint. However, the stop mass is around 150-160 GeV in this region, which is therefore excluded by the lower bound on the stop mass. We also plot in Fig. 3(a), the contour where the NLSP would have a relic density of $\Omega_{\tilde{t}}h^2 = 4 \times 10^{-4}$, if it did not decay. This is shown by the thin green line that lies below the neutralino-stop contour. The small value is a consequence of the strong stop-antistop annihilation cross section.

When we increase $m_{1/2}$, for example to 450 GeV as in panel (b), both m_χ and $m_{\tilde{t}_1}$ are raised and neutralino-stop degeneracy is reached at higher A_0. We see that the $m_{\tilde{t}_1} = 220$ GeV line is closer to the neutralino-stop degeneracy line, and if we kept increasing $m_{1/2}$ we would be able to find points where the stop is lighter than the neutralino and has mass larger than 220 GeV. However, although the Higgs mass constraint also moves to higher A_0, it moves slower than the previous two lines. As a result, there is no overlap region where there is a stop NLSP and the Higgs mass bound is satisfied.

The first two panels in Fig 3 already suggest that there are no allowed regions with a stop NLSP and gravitino LSP in the CMSSM. Generalizing this observation, we first note

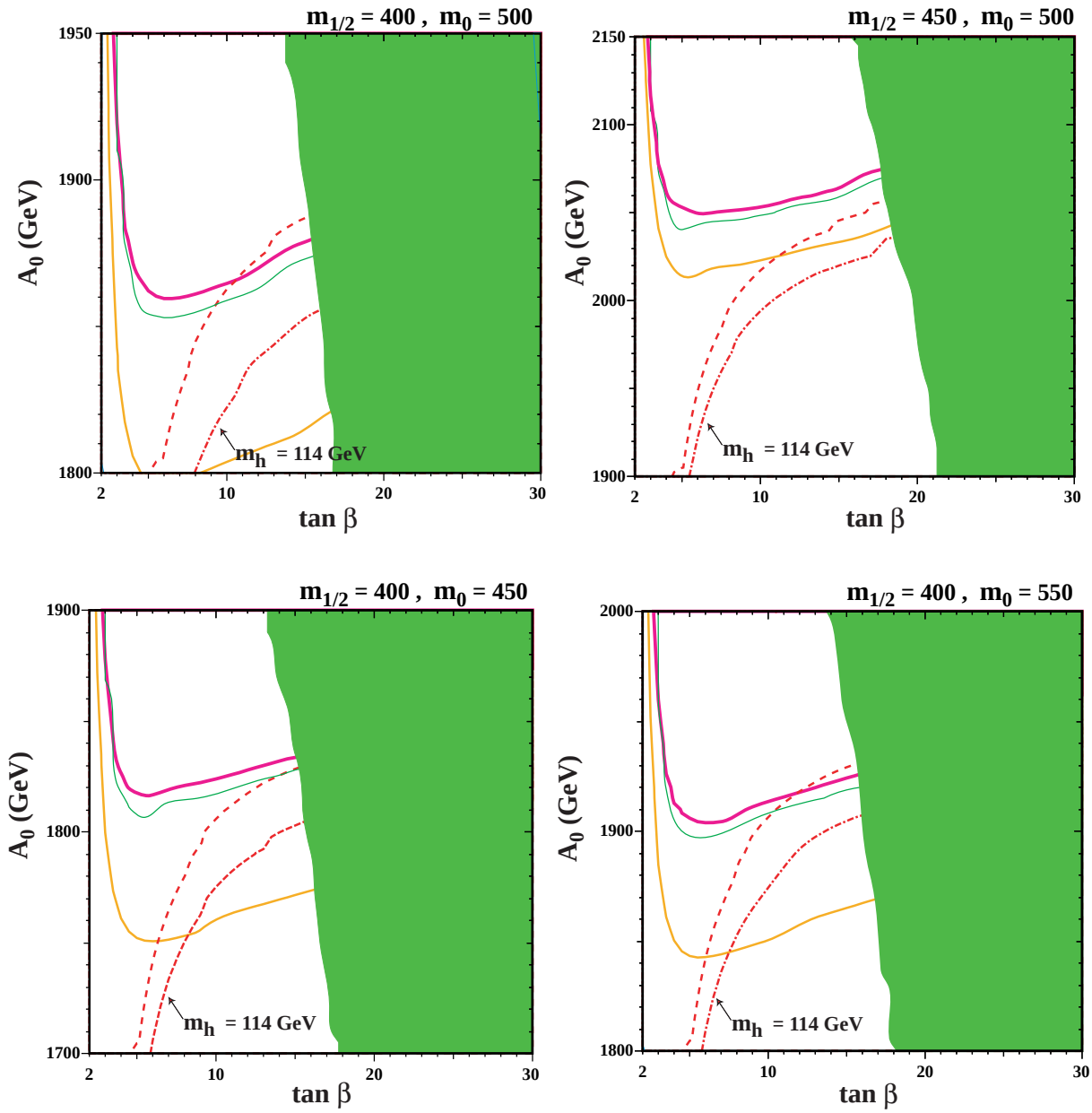

Figure 3: *The* $(\tan\beta, A_0)$ *plane in the CMSSM, for* $(m_{1/2}, m_0)$ *= (a) (400,500) GeV, (b) (450,500) GeV, (c) (400,450) GeV, and (d) (400,550) GeV respectively. We use* $m_t = 171.4$ *GeV,* $m_b(m_b)^{\overline{MS}} = 4.25$ *GeV, and* $\mu > 0$*. The neutralino stop degeneracy contour is plotted as the thick solid purple line: above this line stop is lighter and the NLSP, assuming a light gravitino. The solid orange line is the contour for* $m_{\tilde{t}_1} = 220$ *GeV: above this line, the stop is too light. Large* $\tan\beta$ *is excluded by the* $b \to s\gamma$ *constraint (green shaded region). The Higgs likelihood exclusion line (preferred) is drawn as a dashed red line, while the face value* $m_h = 114.4$ *GeV (deprecated) is the dot-dashed line. Also plotted as the thin green line is the stop relic density* $\Omega_{\tilde{t}} h^2 = 4 \times 10^{-4}$*.*

that, due to the nature of the RGEs in the MSSM, varying m_0 would have less effect than varying $m_{1/2}$. This is shown explicitly by panels (c) and (d) of Fig. 3, which have the same $m_{1/2} = 400$ GeV as in panel (a) but with $m_0 = 450, 550$ GeV respectively. Going from panel (a) to panel (c), the decrease in m_0 results in lower m_h and there is no longer any overlap between the region allowed by m_h and the region where the stop is the NLSP With higher m_0 as in panel (d), we get heavier $\widetilde{t}_L$ and $\widetilde{t}_R$, and hence we need higher X_t and hence A_0 in order to approach $\widetilde{t}_1 - \chi$ degeneracy. However, higher X_t in turn has a problem with the m_h constraint as described above. This illustrates our conclusion that, indeed, a stop NLSP scenario is not possible within the CMSSM.

6 Stop NLSP in the NUHM

We next study the MSSM with non-universal Higgs masses (NUHM) [41]. In the NUHM, the soft supersymmetry-breaking masses in the Higgs sector, m_1 and m_2, are not necessarily equal to the sfermion soft mass m_0 at the GUT scale. Using the radiative electroweak symmetry breaking conditions, we can characterize the new parameters as μ and m_A (the pseudoscalar Higgs mass), both values being defined at the weak scale:

$$\mu^2 \;=\; \frac{m_1^2 + m_2^2 \tan^2\beta + \frac{1}{2}(1 - \tan^2\beta) + \Delta_\mu^{(1)}}{\tan^2\beta - 1 + \Delta_\mu^{(2)}}, \tag{20}$$

and

$$m_A^2(Q) \;=\; m_1^2(Q) + m_2^2(Q) + 2\mu^2(Q) + \Delta_A(Q). \tag{21}$$

Many different sparticles could be the NLSP in this model, in different regions of the NUHM parameter space. These include the lightest neutralino χ, the lighter stau $\tilde{\tau}_1$, the selectron (smuon) $\tilde{e}_R$ ($\tilde{\mu}_R$), the lighter stop $\tilde{t}_1$, the up squark (charm squark) $\tilde{u}_R$ ($\tilde{c}_R$), and the tau sneutrino $\tilde{\nu}_\tau$. Thanks to the RGE, the sbottom tends to be heavier than the stau, so unless we have non-universal soft scalar supersymmetry-breaking masses for squarks and sleptons at the GUT scale, sbottom could not be the NLSP. The up and charm squarks could be the NLSP for very large $|\mu|$ and m_A [42], where the Higgs soft mass-squared m_1^2 or m_2^2 become negative at the GUT scale. However, we discard this possibility, preferring to impose a GUT stability constraint [41]. We also do not consider the other possible NLSPs in this paper, and focus only on the stop.

In order to obtain a light stop, small $|\mu|$ is preferred and, more weakly, large m_A. In Fig. 4(a) we plot various masses as functions of μ for the fixed values $m_A = 1400$ GeV, $\tan\beta = 10$, $A_0 = 2100$ GeV, $m_0 = 500$ GeV (in the region of the values studied previously

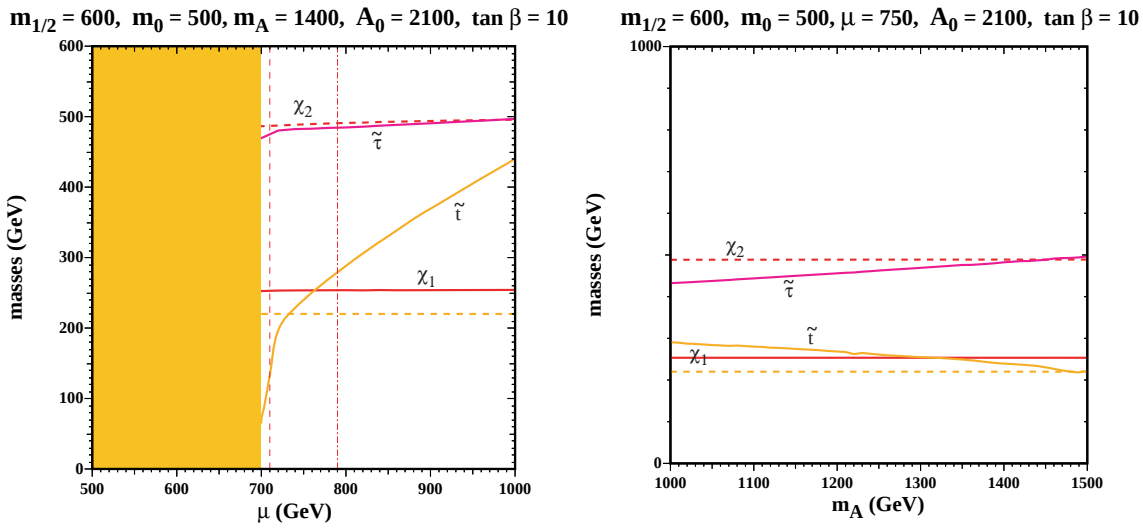

Figure 4: *Sparticle masses in the NUHM as functions of (a) μ with $m_A = 1400$ GeV, and (b) m_A with $\mu = 750$ GeV, both with $\tan\beta = 10$, $A_0 = 2100$ GeV, $m_0 = 500$ GeV and $m_{1/2} = 600$ GeV. We plot the masses of the lightest neutralino (solid red), the second lightest neutralino (dashed red), the lighter stau (purple solid), and the lighter stop (orange solid). In the shaded region, the stop becomes tachyonic. The Higgs likelihood constraint is shown by the vertical dashed red line. We also draw a horizontal dashed line at 220 GeV to indicate the lower bound on the stop mass.*

within the CMSSM) and $m_{1/2} = 600$ GeV (close to the minimum allowed so that $m_\chi > m_{\tilde{t}_1} > 220$ GeV). We see that there is a small range $\mu \simeq 730 - 770$ GeV where the stop is the NLSP and survives the phenomenological constraints. The stop relic density in this region is $\Omega_{\tilde{t}_1} h^2 \sim 10^{-4}$, and the neutralino mass is about 250 GeV. We note that this region is nearly excluded by the Higgs mass constraint. Indeed, if we had taken the LEP limit on m_h at its face value, this region would have been excluded. Panel (b) shows the spectrum as a function of m_A, for $\mu = 750$ GeV. Here we see that $m_{\tilde{t}_1}$ is a decreasing function of m_A, and there is a region where a stop NLSP is allowed, at $m_A \simeq 1350 - 1500$ GeV.

In Fig. 5 we show spectra as functions of (a) $m_{1/2}$, (b) m_0, (c) A_0 and (d) $\tan\beta$. The lightest neutralino, which is bino-like in the cases shown, has a mass that depends essentially on $m_{1/2}$ only. We see that $m_{\tilde{t}_1}$ increases as $m_{1/2}$, m_0 or $\tan\beta$ increases or A_0 decreases, while $m_{\tilde{\tau}}$ increases as $m_{1/2}$, A_0 or $\tan\beta$ decreases or m_0 increases. One might attempt to increase $m_{1/2}$ to obtain a heavier NLSP. However, if we want a stop NLSP, in order to make the stop lighter than neutralino, we need to compensate the increase in $m_{\tilde{t}_1}$ by (say) increasing A_0, but the constraint on $m_{1/2}$ would in turn render it more difficult to satisfy the m_h constraint. We see allowed stop NLSP regions in panel (a) for $m_{1/2} \simeq 595 - 605$ GeV, in

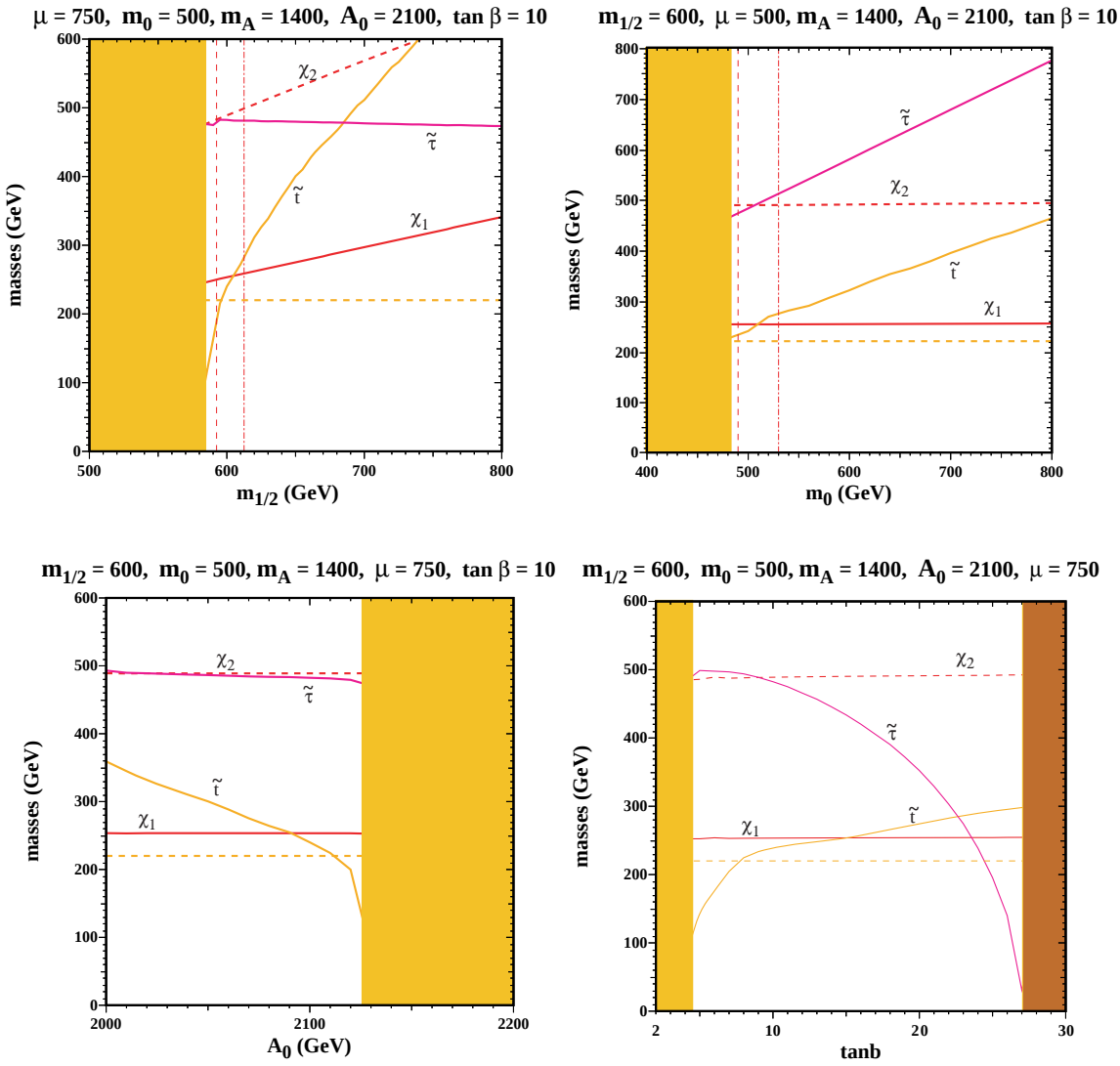

Figure 5: *Sparticle masses in the NUHM as functions of (a) $m_{1/2}$, (b) m_0, (c) A_0 and (d) $\tan\beta$, with other parameter values specified in the legends.*

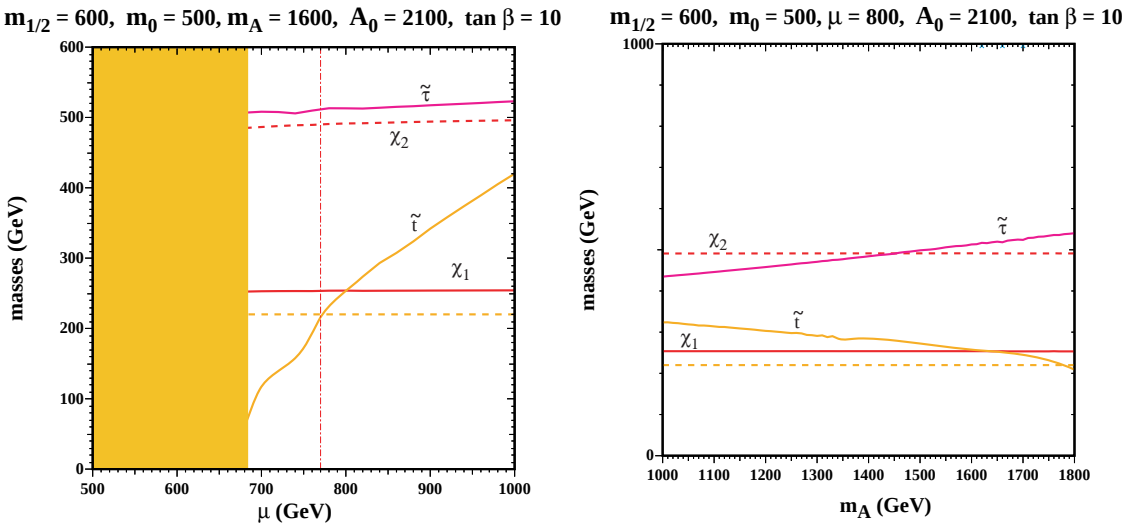

Figure 6: *Same as Fig 4, but with* $m_t = 172.7$ *GeV.*

panel (b) for $m_0 \simeq 490 - 510$ GeV, in panel (c) for $A_0 \simeq 2090 - 2110$ GeV, and in panel (d) for $\tan\beta \simeq 8 - 15$.

It is well known that the Higgs sector is sensitive to the top sector. Therefore, it is instructive compare with the result that would hold if $m_t = 172.7$ GeV (an older experimental value of m_t that is still within one σ of the present central value). We also adjust m_A so as to improve the overlap of the constraints, with the result shown in Fig. 6. We see that the Higgs likelihood constraint becomes as strong as the nominal m_h taken at face value, which is at $\mu \simeq 770$ GeV, and that there is only a tiny region allowed. Thus, postulating a larger m_t does not resolve the dilemma of the Higgs likelihood, even though the face value of m_h is lifted. The allowed region of μ in panel (a) of Fig. 6 is narrower than in the corresponding panel of Fig. 4, and shifted to larger values of μ. Likewise in panel (b), comparison with the corresponding panel of Fig. 4 shows that the allowed region is smaller and shifted to larger values of m_A.

We conclude that there are some small regions of the NUHM parameter space where the $\widetilde{t}_1$ is the NLSP, with a cosmological abundance that would correspond (in the absence of stop decays) to a relic density $\Omega_{\widetilde{t}} h^2 \sim 10^{-4}$. Typical allowed values of the NUHM parameters are $m_{1/2} \sim 600$ GeV, $m_0 \sim 500$ GeV, $A_0 \sim 2100$ GeV, $\mu \sim 750$ GeV, $m_A \sim 1400$ GeV and $\tan\beta \sim 10$. We now discuss the cosmological evolution of such a scenario.

7 Cosmological Evolution of Metastable Stops

We expect the metastable stop squarks and antisquarks density to have frozen out after coannihilation at a temperature $T_F \simeq m_{\tilde{t}_1}/30 \gtrsim 7$ GeV [8], when the age of the Universe $t \sim 10^{-9}$ s [9]. One might have expected a primordial stop-antistop asymmetry comparable to that for conventional baryons, but this would have been eradicated by stop-stop annihilations. The remnant stops and antistops would not have decayed before the next major event in standard Big Bang cosmology, namely the quark-hadron transition when $t \sim 10^{-6}$ to 10^{-5} s. At this point, they would have hadronized into sbaryons, antisbaryons and mesinos.

Simulations and data from relativistic heavy-ion collisions indicate that the relative abundances of hadrons produced at the transition may be modelled by assuming an effective hadronic freeze-out temperature $T_f \simeq 170$ MeV. We recall that all the heavier sbaryons would decay into the lightest $\Lambda_{\widetilde{T}}$ state, which is charged, whereas the mesinos would all decay into the lightest $\widetilde{T}^0$ state, which is relatively harmless. The mass difference between the Λ_b baryon and the $B^{\pm,0}$ mesons is about 365 MeV, and we expect a similar separation for the $\Lambda_{\widetilde{T}}$ sbaryons and the $\widetilde{T}$ mesinos. *Modulo* spin and flavour counting factors, this would suggest a suppression by a factor ~ 10 for the abundance of the sbaryons and antisbaryons relative to the mesinos and antimesinos. This would suggest *a priori* an equivalent relic density $\Omega_{\Lambda_{\widetilde{T}}} h^2 \sim 10^{-5}$, which might have been large enough to change significantly the subsequent abundances of light elements via bound-state effects. The $\Xi^+_{\widetilde{T}}$ state, which is relatively long-lived, would have an abundance about a factor of 3 lower than that of $\Lambda_{\widetilde{T}}$.

It has been argued recently that, following hadronization, stop hadrons $h_{\widetilde{T}}$ would capture each other and form bound states, leading to the further annihilation of stops [27]. The rate for this process is approximately $n_{h_{\widetilde{T}}}(T/m_{\tilde{t}})^{1/2} m_\pi^{-2}$, where $n_{h_{\widetilde{T}}} \simeq \Omega_{h_{\widetilde{T}}} \rho_c / m_{\tilde{t}}$ and $(T/m_{\tilde{t}})^{1/2}$ is the relative velocity in the capture process. The resulting abundance of stop hadrons is determined by equating this annihilation rate to the Hubble expansion rate:

$$\frac{n_{h_{\widetilde{T}}}}{m_\pi^2} \left(\frac{T}{m_{\tilde{t}}} \right)^{1/2} \simeq \sqrt{\frac{8\pi N}{3}} \frac{T^2}{M_P}. \tag{22}$$

This yields a relic $h_{\widetilde{T}}$ number density

$$\frac{n_{h_{\widetilde{T}}}}{n_\gamma} \simeq 80 \frac{m_\pi^2}{M_P} \frac{m_{\tilde{t}}^{1/2}}{T^{3/2}}, \tag{23}$$

[8] Note that the stop has a larger (co)annihilation cross section than does the neutralino, and hence would have smaller freeze out temperature relative to its mass compared to the neutralino with freeze-out temperature of $m_\chi/20$ to $m_\chi/25$.

[9] If the stop-neutralino mass difference is also ~ 5 GeV or smaller, which is quite possible in the allowed NUHM regions found in the previous Section, the stops would have been accompanied by a significant admixture of metastable neutralinos, which we discuss later.

where we use the estimate $N = \mathcal{O}(50)$. The $h_{\widetilde{T}}$ number density is minimized by annihilations at a temperature close to the formation temperature of the bound states, namely $T \sim 200$ MeV, which yield

$$\frac{n_{h_{\widetilde{T}}}}{n_\gamma} \simeq 5 \times 10^{-17}. \tag{24}$$

This corresponds to an effective $\Omega_{h_{\widetilde{T}}} h^2 \sim 2 \times 10^{-6}$ and $\zeta_{h_{\widetilde{T}}} \equiv n_{h_{\widetilde{T}}} m_{h_{\widetilde{T}}}/n_\gamma \simeq 4 \times 10^{-14}$ GeV for $m_{\tilde{t}_1} \sim 200$ GeV. With this abundance, the late decays of stop hadrons would probably not cause problems with light-element abundances, even after allowing for uncertainties in the treatment of showers generated by hadronic decays [10].

However, the catalytic effects of bound states of the negatively-charged metastable relic antisbaryons $\bar{\Lambda}^-_{\widetilde{T}}$ are potentially more dangerous, as emphasized above. Fortunately, as we now show, their abundance would have been suppressed following hadronization and before BBN, by annihilation with conventional baryons to produce $\widetilde{T}$ antimesinos and conventional mesons. The rate for the annihilation of heavy baryons is approximately $n_p m_\pi^{-2}$. Since $n_p \gg n_{\Lambda_{\widetilde{T}}}$ and there is no velocity suppression for this annihilation process, since $\sigma v \to$ constant as $T \to 0$, the rate for annihilation with nucleons would be much larger than the capture process [27] discussed in the previous paragraph. The abundance of antisbaryons would remain in equilibrium until the annihilation rate

$$\eta \frac{n_\gamma}{m_\pi^2} \simeq \frac{1.5 \times 10^{-10} T^3}{m_\pi^2}, \tag{25}$$

where we use $\eta \equiv n_p/n_\gamma = 6.1 \times 10^{-10}$, became of the same order as the expansion rate

$$\sqrt{\frac{8\pi}{3}} \frac{(\Omega_m \rho_c)^{1/2}}{M_P} \simeq \frac{1.2 \times 10^{-4} T^{3/2}}{M_P}, \tag{26}$$

where we use $\Omega_m \sim 0.27$ for the matter density as a fraction of the closure density today. The rates (25) and (26) become comparable when

$$T \simeq 10^2 \left(\frac{m_\pi^2}{M_P} \right)^{2/3} \simeq 0.1 \text{ eV}. \tag{27}$$

The $\bar{\Lambda}^-_{\widetilde{T}}$ abundance would be suppressed by a factor $\exp(-2 \times 10^5)$ already by the time of the onset of BBN at $T \sim 1$ MeV, and the abundance of the dangerous $\bar{\Lambda}^-_{\widetilde{T}}$ state would be driven to an extremely low value $n_{\Lambda_{\widetilde{T}}} \simeq (m_{\tilde{t}} T)^{3/2} e^{-m_{\tilde{t}}/T}$ by the time of freeze-out (27) of annihilations with relic baryons.

[10] We note in passing that the mechanism of [27] ceases to reduce the $\widetilde{T}$ abundance once the temperature falls below about 10 MeV, i.e., after about 10^{-3} s.

The relative abundance of the less dangerous $\Lambda^+_{\widetilde{T}}$ sbaryons would also have been strongly suppressed, as its annihilations with conventional antibaryons would have continued in equilibrium down to temperatures $T \sim 20$ MeV, when

$$\frac{(m_p T)^{3/2} e^{-m_p/T}}{m_\pi^2} \simeq \sqrt{\frac{8\pi N}{3}} \frac{T^2}{M_P}, \tag{28}$$

where $N = \mathcal{O}(10)$ is the number of relativistic degrees of freedom at $T \sim 20$ MeV.

Thus, during and after BBN, one must contend only with the neutral $\widetilde{T}$ mesinos and their antiparticles, with which they mix [30]. Their decays are relatively innocuous, as discussed above. In principle, they might also bind with deuterium to form superheavy nuclei and thus could change the Helium abundance. However, we would not expect the Helium abundance to be greatly affected: it is at the level of 24% of the baryon density and hence has $\Omega_{He} h^2 \sim 0.01$, whereas by the start of BBN the $\widetilde{T}$ mesino density would be down at the 10^{-6} level in the cases that we consider here, so the ratio of the number densities (assuming a $\sim$ 200 GeV stop mass) would be $\mathcal{O}(10^6)$. We note also that the $\widetilde{T}$ mesinos would react with conventional baryons to regenerate $\Lambda^+_{\widetilde{T}}$ sbaryons after their annihilations with antibaryons had frozen out, i.e., at $T < 20$ MeV. However, this process could generate a $\Lambda^+_{\widetilde{T}}$ density of at most 10^{-6}, which would not be problematic.

This analysis therefore finds no cosmological problems with most of the small region of NUHM parameter space discussed in Section 6 where the stop is the NLSP.

8 On the Possibility of a Metastable Neutralino

The conclusion of the previous Section may, however, be modified if the stop NLSP is nearly degenerate with the lightest neutralino χ, a possibility suggested by our analysis of the NUHM parameter space. The χ may decay either into the stop (or antistop) and some other particles: $\chi \to \tilde{t}_1 + X$, $\tilde{t}_1^* + X'$, or into $\widetilde{G} + \gamma$. The latter decay is very slow, being of gravitational strength [4]:

$$\Gamma(\chi \to \widetilde{G}\gamma) = \frac{1}{16\pi} \frac{C^2_{\chi\gamma}}{M_P^2} \frac{m_\chi^5}{m^2_{\widetilde{G}}} \left(1 - \frac{m^2_{\widetilde{G}}}{m^2_\chi}\right)^3 \left(\frac{1}{3} + \frac{m^2_{\widetilde{G}}}{m^2_\chi}\right), \tag{29}$$

where $C_{\chi\gamma} = (O_{1\chi} \cos\theta_W + O_{2\chi} \sin\theta_W)$. The decay rate depends on $m_{\widetilde{G}}$, and for $m_{\widetilde{G}} \simeq 1 - 200$ GeV we get $\Gamma(\chi \to \widetilde{G}\gamma) \simeq 10^{-28} - 10^{-34}$ GeV corresponding to lifetime of $\sim 10^4 - 10^{10}$ s. If the lightest neutralino is almost degenerate with the stop, the two-body decays $\chi \to \widetilde{t}_1 + \bar{t}$, $\bar{\widetilde{t}}_1 + t$, which would be rapid but require a large mass difference $m_\chi - m_{\tilde{t}_1} > m_t$,

are not available. As we discuss below, the decays $\chi \to \tilde{t}_1 + X$, $\tilde{t}_1^* + X'$ may be very suppressed if the χ and $\widetilde{t}_1$ are sufficiently degenerate. If they are suppressed sufficiently for the χ lifetime to exceed about 10^{-5} s, neutralino relics would be present during and after hadronization, and the cosmology of the stops produced in their decays would differ from that of the thermally-produced stops discussed in the previous Section, as we show below.

To show that the abundance of neutralino relics could indeed be significant, recall that when the stop and neutralino are almost degenerate, i.e., $m_\chi - m_{\widetilde{t}_1}$ less than the freeze-out temperature $\sim m_{\widetilde{t}_1}/30$, neutralinos are kept in thermal equilibrium through co-annihilation processes [44] such as $\chi X \leftrightarrow \widetilde{t}_1 X'$ where X, X' are Standard Model particles. We can approximate the neutralino relic density between the epochs of supersymmetric freeze-out and relic decays by

$$\Omega_\chi \simeq \frac{1}{3}\,\Omega_{\widetilde{t}} \simeq 0.25\,\Omega_{NLSP}, \tag{30}$$

modulo the Boltzmann factor from the mass difference. Here the factor 3 is due to colour, and $\Omega_{NLSP} = \Omega_\chi + \Omega_{\widetilde{t}}$ is the relic density one obtains from a standard coannihilation calculation, which leads for near-degenerate χ and $\widetilde{t}_1$ to $\Omega_{NLSP}h^2 \sim 1.6\times10^{-4}$ and hence $\Omega_\chi h^2 \sim 4\times10^{-5}$. Therefore the novel cosmology of the stops produced in neutralino decays is potentially important.

If the $\chi - \widetilde{t}_1$ mass difference is larger than about 1 GeV, the neutralino may decay into three bodies, e.g., $\chi \to \widetilde{t}_1 + \bar{s} + \pi^-$, and into four bodies, e.g., $\chi \to \widetilde{t}_1 + \bar{s} + \ell + \nu$ and conjugate modes, and also into the corresponding final states with $\bar{s} \to \bar{d}$ and/or $\ell + \nu \to q + \bar{q}$. By analogy with the result of [43], the four-body semileptonic decay rate can be approximated as:

$$\Gamma(\chi \to \widetilde{t}_1 \bar{s}\ell\nu) = \mathcal{O}(\frac{1}{100})\frac{G_F^2|V_{ts}|^2}{(2\pi)^5 m_{\tilde{t}_1} m_t^4} \times \left[4|g_L|^2(\delta m)^{10} - 8\,\mathrm{Re}[g_L^* g_R] m_t (\delta m)^9 + 6|g_R|^2 m_t^2 (\delta m)^8)\right], \tag{31}$$

where we allow for both $\widetilde{t}_1$ and $\widetilde{t}_1^*$ modes and a factor of 3 for colour. We have neglected the final-state fermion masses and use

$$g_L = -\frac{g}{\sqrt{2}}\left\{\cos\theta_t\left[O_{\chi 2} + \frac{\sin\theta_W}{3\cos\theta_W}O_{\chi 1}\right] + \sin\theta_t \frac{m_t}{m_W \sin\beta} O_{\chi 4}\right\}, \tag{32}$$

$$g_R = -\frac{g}{\sqrt{2}}\left\{\cos\theta_t \frac{m_t}{m_W \sin\beta} O_{\chi 4} - \sin\theta_t \frac{4\sin\theta_W}{3\cos\theta_W} O_{\chi 1}\right\}, \tag{33}$$

where O is the neutralino diagonalization matrix $O^T M_N O = M_N^{diag}$. We see that the last term in the square bracket in (31) is dominant, due to the large magnitude of m_t. Therefore, we can approximate further to obtain

$$\Gamma(\chi \to \widetilde{t}_1 \bar{s}\ell\nu) \sim \mathcal{O}(\frac{1}{25})\frac{G_F^2|V_{ts}|^2|g_R|^2(\delta m)^8}{(2\pi)^5 m_{\tilde{t}_1} m_t^2}. \tag{34}$$

For $m_{\tilde{t}_1} = 220$ GeV and $\delta m = 1$ GeV, for example, and including the $e\nu, \mu\nu$ and $d\bar{u}$ final states, we estimate $\Gamma(\chi \to \widetilde{t}_1 \bar{s} f \bar{f}) \sim \mathcal{O}(10^{-26})$ GeV, i.e., a χ decay lifetime $\sim 10^2$ s.

The partial decay time would be even longer for yet smaller δm, but it would be necessary to take into account bound-state effects in the $\widetilde{t}_1 \bar{q}$ and $q\bar{q}$ channels, and even in the full four-body final state. A naive scaling by $(\delta m)^8$ would yield a lifetime in excess of 10^{10} s for $\delta m \sim 0.1$ GeV. It is therefore possible that the partial lifetime for $\chi \to \widetilde{t}_1 + X, \tilde{t}_1^* + \bar{X}$ decays could exceed the partial lifetime for $\chi \to \widetilde{G} + \gamma$ decays.

As already remarked, if the χ lifetime exceeds about 10^{-5} s, the $\widetilde{t}_1$ decay products appear after the quark-hadron transition, and the discussion of stop cosmology given in the previous Section must be modified. If τ_χ exceeds about 10^{-3} s, the mechanism of [27] becomes ineffective for reducing the abundance of stop hadrons produced in χ decays, which therefore remain comparable to $\Omega_\chi h^2 \sim 4 \times 10^{-5}$, and also annihilations with antiprotons become ineffective for reducing the $\Lambda^+_{\widetilde{T}}$ abundance. On the other hand, annihilations with baryons remain effective for converting the dangerous $\Lambda^-_{\widetilde{T}}$ sbaryons into relatively innocuous $\widetilde{T}^0$ mesinos for any χ lifetime up to about 10^{14} s. If $\tau_\chi < \tau_{\tilde{t}_1}$, the BBN/CMB constraints on electromagnetic and hadronic stop decays are insensitive to τ_χ, and depend only on $\tau_{\tilde{t}_1}$. If $\tau_\chi > \tau_{\tilde{t}_1}$, the the BBN/CMB constraints on electromagnetic and hadronic stop decays should be evaluated with $\tau_{\tilde{t}_1}$ replaced by τ_χ. Finally, if the partial lifetime for $\chi \to \widetilde{t}_1 + X, \tilde{t}_1^* + \bar{X}$ decays exceeds that for $\chi \to \widetilde{G} + \gamma$ decays, the χ decay contribution to the relic stop density is diluted by the ratio of the partial decay rates.

We therefore distinguish five metastable neutralino cases.

1. If $\tau_\chi < 10^{-3}$ s, the residual suppression of the $\widetilde{T}^0$ mesino density the mechanism of [27] may still be sufficient to evade the BBN/CMB constraints on electromagnetic and hadronic stop decays.

2. If 10^{-3} s $< \tau_\chi < 10^4$ s, the the mechanism of [27] is ineffective, and the indirectly-produced $\widetilde{T}^0$ mesinos still have $\Omega_\chi h^2 \sim 4 \times 10^{-5}$. Since the neutralinos decay before the epoch when the light-element abundances constrain the electromagnetic and hadronic stop decays, these depend on the value of $\tau_{\tilde{t}_1}$ in the usual way. The relic density of $\widetilde{T}^0$ mesinos respects the limit obtained in [16] by considering electromagnetic decays, but not the hadronic limit given in [15], which will be re-evaluated in [45].

3. The usual light-element abundance constraints also apply if 10^4 s $< \tau_\chi < \tau_{\tilde{t}_1}$, and the relic density of $\widetilde{T}^0$ mesinos is again marginal.

4. If $\tau_\chi > \tau_{\tilde{t}_1}$ and 10^4 s simultaneously, the usual light-element abundance constraints

still apply, but they should be evaluated with $\tau_{\tilde{t}_1}$ replaced by $\tau_\chi + \tau_{\tilde{t}_1}$. In addition, we should consider also the effect of neutralino decay itself to the light element abundance.

5. In both the last two cases, the scenario may survive more easily if the partial lifetime for $\chi \to \widetilde{t}_1 + X, \tilde{t}_1^* + \bar{X}$ decays exceeds that for $\chi \to \widetilde{G} + \gamma$ decays, in which case the abundance of $\widetilde{T}^0$ mesinos is suppressed by the ratio of the partial decay rates.

9 Summary

The scenario of gravitino dark matter with a stop NLSP has rich phenomenology, for both collider experiments and cosmology. Unfortunately this scenario is disfavoured in the CMSSM and NUHM, due to the existing collider limits and the close relation between the masses of the light stop and the light Higgs boson. However, we find that there could still be a small allowed region, at least within the NUHM, with $m_{1/2} \sim 600$ GeV, $m_0 \sim 500$ GeV, $A_0 \sim 2100$ GeV, $\mu \sim 750$ GeV, $m_A \sim 1400$ GeV and $\tan\beta \sim 10$.

Much of the discussion in this paper on the stop NLSP scenario could be applied as well to a scharm or sup NLSP in more general MSSM models with a gravitino LSP. In such a case, we expect that the Higgs constraint would be less stringent. Presumably the late production of the NLSP would be less important since, with the light u, c quarks in place of the heavy t quark, two-body decay channels would probably be available, unless the mass difference between neutralino and the NLSP is very small (less than $m_{u,c}$), in which case the neutralino would decay directly into the gravitino. The case of a sbottom NLSP would in this respect be intermediate between the stop and scharm cases. However, as noted above, the lightest mesino would, in this case, probably be charged, and hence capable of bound-state catalysis of dangerous light-element transmutations.

For a possible realization of models with a sup NLSP, see [42], where one could get light scharm and sup in the NUHM by assuming very high values for μ and m_A, which would mean violating the GUT stability constraint. Another possiblity would be to postulate non-universality between the first two generations and the third, and between squarks and sleptons. It is interesting to note that the suppression of the lighter squark eigenmass via diagonalization is much less for sup than for stop, so it is not necessary to postulate large A_0 in these scenarios.

As Hamlet said: 'There are more things in Heaven and Earth, Horatio, than are dreamt of in your philosophy.' This comment certainly applies to supersymmetric phenomenology. There are surely many important aspects of the stop NLSP scenario that we have overlooked

in this paper, and many other NLSP candidates could be envisaged, beyond the stop, the neutralino and the stau, which are the three options usually considered. If supersymmetry is the 'surprise' most expected at the LHC, one should perhaps expect it to appear in an unexpected way. The dominant signature might not be the 'expected' missing transverse energy, but rather some brand of metastable charged particle, which could well have strong interactions, like the stop considered here.

Acknowledgments

The work of K.A.O. was supported in part by DOE grant DE–FG02–94ER–40823. The work of Y.S. was supported in part by the NSERC of Canada. J.L. D.-C. thanks SNI and CONACYT (Mexico) for their support, and the HELEN project for financing a visit to CERN. JE is pleased to thank Oleg Lebedev for useful discussions, and YS is pleased to thank Maxim Pospelov and Rich Cyburt for useful discussions. We thank Teruki Kamon for information on the CDF search on (meta)stable charged massive particles.

Appendix: Three-Body Stop Decays

We present in this Appendix some details of the calculation of the three-body stop decay, using the following notations. For the top contribution, we introduce:

$$A_{\tilde{t}} \equiv \frac{1}{2}(\cos\theta_{\tilde{t}} + \sin\theta_{\tilde{t}}), \tag{35}$$

$$B_{\tilde{t}} \equiv \frac{1}{2}(\cos\theta_{\tilde{t}} - \sin\theta_{\tilde{t}}). \tag{36}$$

and for the sbottom contribution we introduce:

$$a_i \equiv (\sin\theta_{\tilde{b}}, \cos\theta_{\tilde{b}}), \tag{37}$$

$$b_i \equiv (\cos\theta_{\tilde{b}}, -\sin\theta_{\tilde{b}}). \tag{38}$$

We also define

$$\kappa_i \equiv (\cos\theta_{\tilde{t}}\cos\theta_{\tilde{b}}, -\cos\theta_{\tilde{t}}\cos\theta_{\tilde{b}}). \tag{39}$$

In the chargino contribution we have:

$$V_i \equiv \frac{1}{2}(V_{i2}\sin\beta + U_{i2}\cos\beta), \tag{40}$$

$$A_i \equiv \frac{1}{2}(V_{i2}\sin\beta - U_{i2}\cos\beta), \tag{41}$$

and for the low-to-moderate range of $\tan\beta$ we have:

$$2S_1 = -g_2\cos\phi_L + \frac{g_2 m_t \sin\phi_L \sin\theta_{\tilde{t}}}{\sqrt{2}m_W \sin\beta} \quad (42)$$

$$2P_1 = -g_2\cos\phi_L - \frac{g_2 m_t \sin\phi_L \sin\theta_{\tilde{t}}}{\sqrt{2}m_W \sin\beta} \quad (43)$$

where $\cos\phi_L, \pm\sin\phi_L$ are elements of the matrix V that diagonalizes the chargino mass matrix, and expressions for S_2 and P_2 may be obtained by replacing $\cos\phi_L \to -\sin\phi_L$ and $\sin\phi_L \to \cos\phi_L$ in the last equations.

For the *square of the top contribution* to the decay amplitude, we have:

$$W_{tt} = \frac{4}{m_W^2 m_{\widetilde{G}}^2} h_1[h_2((A_{\tilde{t}}+B_{\tilde{t}})^2 m_t^2 + (A_{\tilde{t}}-B_{\tilde{t}})^2 q_1^2) + h_3((A_{\tilde{t}}^2 - B_{\tilde{t}}^2) m_{\widetilde{G}} m_t + (A_{\tilde{t}}-B_{\tilde{t}})^2 (f_2 - m_{\widetilde{G}}^2))], \quad (44)$$

where

$$h_1 = m_{\tilde{t}_1}^2 m_{\widetilde{G}}^2 - f_2^2, \quad (45)$$

$$h_2 = -2f_1 f_3 + 2f_3^2 + m_W^2(-f_2 + 3f_3 + m_{\widetilde{G}}^2), \quad (46)$$

$$h_3 = -2m_W^2 q_1^2 - 2(f_1 - f_3)(2f_1 - 2f_3 - 3m_W^2). \quad (47)$$

From the energies $E_1 = p_1^0$ and $E_W = k^0$, we can define variables x, y by $E_1 = m_{\tilde{t}_1}^2 x/2$ and $E_W = m_{\tilde{t}_1}^2 y/2$. In turn, this allows to express all the inner products of momenta that appear in the functions W_{ii} in terms of x and y. Then, $q_1^2 = m_{\tilde{t}_1}^2(1 + r_1 - x)$ and the functions f_i are given as follows:

$$f_1 = \frac{m_{\tilde{t}_1}^2}{2} y, \quad (48)$$

$$f_2 = \frac{m_{\tilde{t}_1}^2}{2} x, \quad (49)$$

$$f_3 = \frac{m_{\tilde{t}_1}^2}{2}(-1 - r_1 - r_2 + x + y). \quad (50)$$

where $r_1 = m_{\widetilde{G}}^2/m_{\tilde{t}_1}^2$, $r_2 = m_W^2/m_{\tilde{t}_1}^2$.

Similar expressions can be written for the *square of the sbottom contribution* to the decay amplitude, namely:

$$|M_{\tilde{b}}|^2 = \sum_{i,j} C_{\tilde{b}_i}^* C_{\tilde{b}_j} P_{\tilde{b}_i}^*(q_2) P_{\tilde{b}_j}(q_2) W_{\tilde{b}_i \tilde{b}_j} \quad (51)$$

where:

$$W_{\tilde{b}_i \tilde{b}_j} = \frac{16}{3}\frac{a_i a_j + b_i b_j}{m_W^2 m_{\widetilde{G}}^2}(m_{\tilde{t}_1}^2 m_W^2 - f_1^2)(q_2^2 m_{\widetilde{G}}^2 - (q_2.p_1)^2)\, p_1.p_2 \quad (52)$$

and: $q_2^2 = m_{\tilde{t}_1}^2(1 + r_2 - y)$, $q_2.p_1 = f_2 - f_3$ and $p_1.p_2 = f_2 - f_3 - m_{\widetilde{G}}^2$.

The *square of the chargino contribution* takes the form:

$$|M_{\chi^+}|^2 = \sum_{i,j} C_{\chi^+}^2 P_{\chi_i^+}^*(q_3) P_{\chi_j^+}(q_3) W_{\chi_i^+\chi_j^+} \tag{53}$$

where

$$W_{\chi_i^+\chi_j^+} = \frac{32}{3m_W^2 m_{\widetilde{G}}^2}(2m_W^2 m_{\widetilde{G}}^2 + f_3^2)\left[2f_4(\Sigma_{(1)ij} m_{\widetilde{G}} m_\chi + \Sigma_{(2)ij} f_5) + p_1.p_2\,(m_\chi^2 \Sigma_{(3)ij} - q_3^2 \Sigma_{(2)ij})\right] \tag{54}$$

and $q_3^2 = m_{\widetilde{G}}^2 + m_W^2 + 2f_3$, $f_4 = (m_{\tilde{t}_1}^2/2)(2 - x - y)$, $f_5 = f_3 + m_{\widetilde{G}}^2$. Also, we define $\Sigma_{(1)ij} \equiv (A_iA_j - V_iV_j)(S_iS_j + P_iP_j)$, $\Sigma_{(2)ij} \equiv (A_iA_j + V_iV_j)(S_iS_j + P_iP_j) - (A_iV_j + V_iA_j)(S_iP_j + P_iS_j)$, and $\Sigma_{(3)ij} = (A_iA_j + V_iV_j)(S_iS_j + P_iP_j) + (A_iV_j + V_iA_j)(S_iP_j + P_iS_j)$.

The *interference between the top and chargino contributions* leads to the following expression for $W_{t\chi^+}$:

$$W_{t\chi_i^+} = 2(T_{1i} - m_t T_{2i}) + 2m_{\chi_i^+}(T_{3i} - m_t T_{4i}) - \frac{2}{3}(T_{5i} - m_t T_{6i}) - \frac{2m_{\chi_i^+}}{3}(T_{7i} - m_t T_{8i}) \tag{55}$$

The functions T_i may be written as follows:

$$\begin{aligned}
T_{1i} &= \frac{4\,\alpha_{1i}}{m_{\widetilde{G}} m_W^2}[-2f_1^3 m_{\widetilde{G}}^2 + (f_2 f_3^2 - m_{\widetilde{G}}^2 f_1 f_3)h_4 - 2f_1 f_2 f_3(-f_2 + 2f_3 + m_{\widetilde{G}}^2) \\
&\quad -2f_2^3 m_W^2 + f_2 m_W^2(f_3^2 + 2m_{\widetilde{G}}^2 m_{\tilde{t}_1}^2) - f_1 m_W^2(2f_2^2 + f_2 f_3 + m_{\widetilde{G}}^2 f_3 - 2m_{\widetilde{G}}^2 m_{\tilde{t}_1}^2) \\
&\quad +m_W^2(f_2^2 - m_{\widetilde{G}}^2 m_{\tilde{t}_1}^2)h_5 + f_1^2(2f_2 f_3 - 2m_{\widetilde{G}}^2 f_2 + m_{\widetilde{G}}^2(4f_3 + 2m_{\widetilde{G}}^2 + m_W^2))], \qquad (56) \\
T_{2i} &= \frac{4\,\alpha_{2i}}{m_{\widetilde{G}}^2 m_W^2}[(f_1 - f_3)(2f_3 + m_{\widetilde{G}}^2)(m_{\widetilde{G}}^2 f_1 - f_2 f_3) \\
&\quad +m_W^2(-f_2 f_3^2 - f_2^2(f_3 + m_{\widetilde{G}}^2) + m_{\widetilde{G}}^2(f_1 f_3 + f_3 m_{\tilde{t}_1}^2 + m_{\widetilde{G}}^2 m_{\tilde{t}_1}^2))], \qquad (57) \\
T_{3i} &= \frac{4\,\alpha_{3i}}{m_{\widetilde{G}}^2 m_W^2}[2f_1^2 m_{\widetilde{G}}^2(m_{\widetilde{G}}^2 - f_2) + f_2 f_3^2(m_{\widetilde{G}}^2 - m_{\tilde{t}_1}^2) \\
&\quad +f_1 f_3(2f_2^2 - 2f_2 m_{\widetilde{G}}^2 - m_{\widetilde{G}}^4 + m_{\widetilde{G}}^2 m_{\tilde{t}_1}^2) \\
&\quad -m_W^2(f_2^2 - m_{\widetilde{G}}^2 m_{\tilde{t}_1}^2)(2f_2 - f_3 - 2m_{\widetilde{G}}^2)], \qquad (58)
\end{aligned}$$

$$
\begin{aligned}
T_{4i} &= -\frac{4\,\alpha_{4i}}{m_{\widetilde{G}} m_W^2}[(f_1-f_3)(m_{\widetilde{G}}^2 f_1 - f_2 f_3) + m_W^2(f_2^2 - m_{\widetilde{G}}^2 m_{\tilde{t}_1}^2)], && (59)\\
T_{5i} &= \frac{4\,\alpha_{1i}}{m_{\widetilde{G}} m_W^2}[-2f_1^2(f_2 - m_{\widetilde{G}}^2)(f_3 + m_{\widetilde{G}}^2) + f_3^2 f_2(2f_3 + m_{\widetilde{G}}^2) - f_3^2 m_{\tilde{t}_1}^2(f_2 + 2f_3)\\
&\quad + f_1 f_3(2f_2^2 - 2m_{\widetilde{G}}^2 f_2 - (2f_3 + m_{\widetilde{G}}^2)(m_{\widetilde{G}}^2 - m_{\tilde{t}_1}^2))\\
&\quad + m_W^2 f_2(-2f_2^2 + 5f_2 f_3 + f_3^2 + 2m_{\widetilde{G}}^2 f_2)\\
&\quad - m_W^2 m_{\tilde{t}_1}^2(2f_2(f_3 - m_{\widetilde{G}}^2) + (f_3 + m_{\widetilde{G}}^2)(f_3 + 2m_{\widetilde{G}}^2))\\
&\quad m_W^2 f_1(f_2(f_3 - 2m_{\widetilde{G}}^2) - m_{\widetilde{G}}^2(f_3 - 2m_{\tilde{t}_1}^2)) + 2m_W^4(f_2^2 - m_{\widetilde{G}}^2 m_{\tilde{t}_1}^2)], && (60)\\
T_{6i} &= \frac{4\,\alpha_{2i}}{m_{\widetilde{G}}^2 m_W^2}[-2f_1^2 m_{\widetilde{G}}^2(f_3 + m_{\widetilde{G}}^2) + m_W^2 m_{\widetilde{G}}^2 f_1(2f_2 + f_3)\\
&\quad + f_1 f_3(2f_2 f_3 + m_{\widetilde{G}}^2(3f_2 + 2f_3) + m_{\widetilde{G}}^4)\\
&\quad + f_3(-m_W^2 f_2^2 - m_{\widetilde{G}}^2 m_{\tilde{t}_1}^2(f_3 + m_W^2) - f_2 f_3(2f_3 + m_{\widetilde{G}}^2 + m_W^2))], && (61)\\
T_{7i} &= \frac{4\,\alpha_{3i}}{m_{\widetilde{G}}^2 m_W^2}[f_1^2(-2m_{\widetilde{G}}^2 f_2 + 2m_{\widetilde{G}}^4) + f_2 f_3^2(m_{\widetilde{G}}^2 - m_{\tilde{t}_1}^2)\\
&\quad + f_1 f_3(2f_2^2 - 2f_2 m_{\widetilde{G}}^2 - m_{\widetilde{G}}^4 + m_{\widetilde{G}}^2 m_{\tilde{t}_1}^2),\\
&\quad - f_2 m_W^2(f_2(2f_2 - f_3) - 2m_{\widetilde{G}}^2(f_2 + f_3)) - m_{\widetilde{G}}^2 m_{\tilde{t}_1}^2 m_W^2(-2f_2 + 3f_3 + 2m_{\widetilde{G}}^2)], && (62)\\
T_{8i} &= \frac{4\,\alpha_{4i}}{m_{\widetilde{G}} m_W^2}[2m_{\widetilde{G}}^2 f_1^2 + f_3(f_2 f_3 + f_3 m_{\tilde{t}_1}^2 + 2f_2 m_W^2) - f_1(3f_2 f_3 + m_{\widetilde{G}}^2(f_3 + 2m_W^2))], && (63)
\end{aligned}
$$

where $\alpha_{1i} = \Delta_{3i}A_{\tilde{t}} + \Delta_{4i}B_{\tilde{t}}$, $\alpha_{2i} = \Delta_{3i}A_{\tilde{t}} - \Delta_{4i}B_{\tilde{t}}$, $\alpha_{3i} = \Sigma_{3i}A_{\tilde{t}} + \Sigma_{4i}B_{\tilde{t}}$, $\alpha_{4i} = \Sigma_{3i}A_{\tilde{t}} - \Sigma_{4i}B_{\tilde{t}}$, with $\Delta_{3i} = V_iS_i - A_iP_i$, $\Sigma_{3i} = V_iS_i + A_iP_i$ and $\Delta_{4i} = V_iP_i - A_iS_i$, $\Sigma_{4i} = V_iP_i + A_iS_i$. We also denote $h_4 = 2f_3 + m_{\widetilde{G}}^2 - m_{\tilde{t}_1}^2$, $h_5 = 3f_3 + 2m_{\widetilde{G}}^2 + m_W^2$.

The *interference between the top and sbottom contributions*, $W_{t\tilde{b}}$ may be written as:

$$
W_{t\tilde{b}_i} = \frac{(f_2\, q_2.q_1 - p.q_2 m_{\widetilde{G}}^2)}{m_{\widetilde{G}}^2 m_W^2}[m_W^2 Y_{1pi} - f_1 Y_{1ki}] + \frac{1}{3m_W^2}[m_W^2 Y_{2pi} - f_1 Y_{2ki}], \qquad (64)
$$

where

$$
\begin{aligned}
Y_{1pi} &= 4\,Z_{1i}[(f_1+f_2)m_{\widetilde{G}}^2+(f_2-f_3-2m_{\widetilde{G}}^2)m_{\tilde{t}_1}^2] \\
&\quad -4\,Z_{2i}[(f_1+f_2-m_{\tilde{t}_1}^2)m_t m_{\widetilde{G}}], \qquad (65)\\
Y_{1ki} &= 4\,Z_{1i}[2f_1(f_2-m_{\widetilde{G}}^2)+f_3(m_{\widetilde{G}}^2-m_{\tilde{t}_1}^2)+m_W^2(-f_2+m_{\widetilde{G}}^2)] \\
&\quad -4\,Z_{2i}[(-f_1+f_3-m_W^2)m_t m_{\widetilde{G}}], \qquad (66)\\
Y_{2pi} &= \frac{4\,Z_{1i}}{m_{\widetilde{G}}^2}[f_3^3(m_{\widetilde{G}}^2+m_{\tilde{t}_1}^2)+f_2 m_{\tilde{t}_1}^2(f_3^2+2f_3m_{\widetilde{G}}^2-m_{\widetilde{G}}^2(m_{\widetilde{G}}^2+m_{\tilde{t}_1}^2)) \\
&\quad +m_{\widetilde{G}}^2 m_{\tilde{t}_1}^2(-f_3^2+f_3m_{\tilde{t}_1}^2+m_{\widetilde{G}}^2(2m_{\tilde{t}_1}^2+m_W^2)) \\
&\quad -f_2^2(f_3(m_{\widetilde{G}}^2+2m_{\tilde{t}_1}^2)+m_{\widetilde{G}}^2(2m_{\tilde{t}_1}^2+m_W^2)) \\
&\quad +m_{\widetilde{G}}^2 f_1(f_2(f_2+f_3+m_{\widetilde{G}}^2)+m_{\tilde{t}_1}^2(f_2-f_3-3m_{\widetilde{G}}^2))] \\
&\quad +\frac{4\,Z_{2i}}{m_{\widetilde{G}}^2}[m_{\widetilde{G}}m_t(-f_3^3-f_2m_{\tilde{t}_1}^2(f_3-m_{\widetilde{G}}^2) \\
&\quad +f_2^2(f_3+m_{\tilde{t}_1}^2+m_W^2)+m_{\tilde{t}_1}^2(f_3^2-m_{\widetilde{G}}^2(m_{\tilde{t}_1}^2+m_W^2)) \\
&\quad +m_{\widetilde{G}}m_t f_1(-f_2(f_2+f_3+m_{\widetilde{G}}^2)+2m_{\widetilde{G}}^2m_{\tilde{t}_1}^2)], \qquad (67)\\
Y_{2ki} &= \frac{4\,Z_{1i}}{m_{\widetilde{G}}^2}[(f_2^2-f_2f_3-m_{\widetilde{G}}^2m_{\tilde{t}_1}^2)(f_3(-m_{\widetilde{G}}^2+m_{\tilde{t}_1}^2)+m_W^2(f_2-m_{\widetilde{G}}^2)) \\
&\quad -f_1(2f_2^3-2f_2^2(f_3+m_{\widetilde{G}}^2)+m_{\widetilde{G}}^2f_3(m_{\widetilde{G}}^2-m_{\tilde{t}_1}^2) \\
&\quad +m_{\widetilde{G}}^2f_2(2f_3-2m_{\tilde{t}_1}^2-m_W^2)+m_{\widetilde{G}}^4(2m_{\tilde{t}_1}^2+m_W^2)) \\
&\quad -2m_{\widetilde{G}}^2f_1^2(f_2-m_{\widetilde{G}}^2)] \\
&\quad +\frac{4\,Z_{2i}}{m_{\widetilde{G}}^2}[-f_3m_{\widetilde{G}}m_t(-f_2^2+(f_3+m_{\widetilde{G}}^2)m_{\tilde{t}_1}^2+f_2(f_3+m_W^2)) \\
&\quad +f_1m_{\widetilde{G}}m_t(-f_2^2+3f_2f_3+m_{\widetilde{G}}^2(f_3+m_{\tilde{t}_1}^2+m_W^2)-2f_1m_{\widetilde{G}}^2)], \qquad (68)
\end{aligned}
$$

and $Z_{1i}=A_{\tilde{t}}\Sigma_{5i}+B_{\tilde{t}}\Delta_{5i}$, $Z_{2i}=A_{\tilde{t}}\Sigma_{5i}-B_{\tilde{t}}\Delta_{5i}$, $\Sigma_{5i}=(a_i+b_i)/2$, and $\Delta_{5i}=(a_i-b_i)/2$.

Finally, the *interference between the chargino and sbottom contributions* is given by:

$$W_{\chi_i^+\tilde{b}_j}=2[X_{1pij}-m_{\chi_i^+}X_{2pij}]-\frac{2}{3}[X_{1kij}-m_{\chi_i^+}X_{2kij}] \qquad (69)$$

where

$$X_{1pij} = -\frac{4\,\sigma_{1ij}}{m_{\widetilde{G}} m_W^2}[(-f_1 - f_2 + 2f_3 + m_{\widetilde{G}}^2 + m_W^2)(h_6 + h_7 - m_{\widetilde{G}}^2 f_1^2)], \tag{70}$$

$$\begin{aligned} X_{1kij} = & -\frac{4\,\sigma_{1ij}}{m_{\widetilde{G}} m_W^2}[f_1^2(f_3(f_2+f_3) + m_{\widetilde{G}}^2(f_2 - 2f_3) - m_{\widetilde{G}}^4) \\ & -f_1 f_3(f_2^2 - f_2(3f_3 + m_{\widetilde{G}}^2 - 2m_W^2) + f_3(2f_3 + m_{\widetilde{G}}^2 + m_{\tilde{t}_1}^2 + m_W^2)) \\ & +m_W^2(f_2^3 - f_2^2(3f_3 + m_{\widetilde{G}}^2) + (f_3 + m_{\widetilde{G}}^2)^2 m_{\tilde{t}_1}^2 + f_2(2f_3^2 - m_{\widetilde{G}}^2 m_{\tilde{t}_1}^2 + f_3(m_{\widetilde{G}}^2 + m_W^2)))], \end{aligned} \tag{71}$$

$$X_{2pij} = -\frac{4\,\sigma_{2ij}}{m_{\widetilde{G}}^2 m_W^2}(-f_2 + f_3 + m_{\widetilde{G}}^2)[h_6 + h_7 - f_1^2 m_{\widetilde{G}}^2], \tag{72}$$

$$X_{2kij} = -\frac{4\,\sigma_{2ij}}{m_{\widetilde{G}}^2 m_W^2}(-f_2 + f_3 + m_{\widetilde{G}}^2)[h_6 + h_7 - f_1^2 m_{\widetilde{G}}^2], \tag{73}$$

and $h_6 = f_1 f_3(f_2 - f_3)$, $h_7 = m_W^2(f_2(-f_2 + f_3) + m_{\widetilde{G}}^2 m_{\tilde{t}_1}^2)$, and $\sigma_{1ij} = \Gamma_{1ij} V_i - \Gamma_{2ij} A_i$, $\sigma_{2ij} = \Gamma_{1ij} V_i + \Gamma_{2ij} A_i$. We also define $\Gamma_{1j} = \Sigma_{5j} S_i + \Delta_{5j} P_i$, $\Gamma_{2ij} = \Sigma_{5j} P_i + \Delta_{5j} S_i$, with Σ_{5j}, Δ_{5j} defined previously.

References

[1] J. Ellis, J.S. Hagelin, D.V. Nanopoulos, K.A. Olive and M. Srednicki, Nucl. Phys. B **238** (1984) 453; see also H. Goldberg, Phys. Rev. Lett. **50** (1983) 1419.

[2] T. Falk, K. A. Olive and M. Srednicki, Phys. Lett. B **339** (1994) 248 [arXiv:hep-ph/9409270].

[3] J. R. Ellis, K. A. Olive, Y. Santoso and V. C. Spanos, Phys. Rev. D **70**, 055005 (2004) [arXiv:hep-ph/0405110].

[4] J. R. Ellis, K. A. Olive, Y. Santoso and V. C. Spanos, Phys. Lett. B **588** (2004) 7 [arXiv:hep-ph/0312262].

[5] J. L. Feng, A. Rajaraman and F. Takayama, Phys. Rev. Lett. **91** (2003) 011302 [arXiv:hep-ph/0302215]; Phys. Rev. D **68** (2003) 063504 [arXiv:hep-ph/0306024].

[6] J. L. Feng, S. Su and F. Takayama, Phys. Rev. D **70** (2004) 075019 [arXiv:hep-ph/0404231].

[7] J. L. Feng, S. f. Su and F. Takayama, Phys. Rev. D **70** (2004) 063514 [arXiv:hep-ph/0404198].

[8] K. Kohri, T. Moroi and A. Yotsuyanagi, Phys. Rev. D **73** (2006) 123511 [arXiv:hep-ph/0507245].

[9] K. Jedamzik, K. Y. Choi, L. Roszkowski and R. Ruiz de Austri, JCAP **0607** (2006) 007 [arXiv:hep-ph/0512044]; D. G. Cerdeno, K. Y. Choi, K. Jedamzik, L. Roszkowski and R. Ruiz de Austri, JCAP **0606** (2006) 005 [arXiv:hep-ph/0509275].

[10] F. D. Steffen, JCAP **0609**, 001 (2006) [arXiv:hep-ph/0605306].

[11] A. De Roeck, J. R. Ellis, F. Gianotti, F. Moortgat, K. A. Olive and L. Pape, arXiv:hep-ph/0508198.

[12] J. R. Ellis, A. R. Raklev and O. K. Oye, JHEP **0610**, 061 (2006) [arXiv:hep-ph/0607261].

[13] J. L. Feng and B. T. Smith, Phys. Rev. D **71** (2005) 015004 [Erratum-ibid. D **71** (2005) 0109904] [arXiv:hep-ph/0409278].

[14] K. Hamaguchi, Y. Kuno, T. Nakaya and M. M. Nojiri, Phys. Rev. D **70** (2004) 115007 [arXiv:hep-ph/0409248].

[15] E. Holtmann, M. Kawasaki, K. Kohri and T. Moroi, Phys. Rev. D **60**, 023506 (1999) [arXiv:hep-ph/9805405]; M. Kawasaki, K. Kohri and T. Moroi, Phys. Rev. D **63** (2001) 103502 [arXiv:hep-ph/0012279]; K. Kohri, Phys. Rev. D **64** (2001) 043515 [arXiv:astro-ph/0103411].

[16] R. H. Cyburt, J. R. Ellis, B. D. Fields and K. A. Olive, Phys. Rev. D **67** (2003) 103521 [arXiv:astro-ph/0211258].

[17] J. R. Ellis, K. A. Olive and E. Vangioni, Phys. Lett. B **619** (2005) 30 [arXiv:astro-ph/0503023].

[18] M. Kawasaki, K. Kohri and T. Moroi, Phys. Lett. B **625** (2005) 7 [arXiv:astro-ph/0402490]; Phys. Rev. D **71** (2005) 083502 [arXiv:astro-ph/0408426].

[19] M. Pospelov, arXiv:hep-ph/0605215.

[20] K. Kohri and F. Takayama, arXiv:hep-ph/0611016; M. Kaplinghat and A. Rajaraman, Phys. Rev. D **74** (2006) 103004 [arXiv:astro-ph/0606209].

[21] R. H. Cyburt, J. Ellis, B. D. Fields, K. A. Olive and V. C. Spanos, JCAP **0611** (2006) 014 [arXiv:astro-ph/0608562].

[22] T. Kanzaki, M. Kawasaki, K. Kohri and T. Moroi, arXiv:hep-ph/0609246.

[23] J. R. Ellis and S. Rudaz, Phys. Lett. B **128** (1983) 248.

[24] C. Boehm, A. Djouadi and M. Drees, Phys. Rev. D **62** (2000) 035012 [arXiv:hep-ph/9911496].

[25] J. R. Ellis, K. A. Olive and Y. Santoso, Astropart. Phys. **18** (2003) 395 [arXiv:hep-ph/0112113].

[26] T. Phillips, talk at DPF 2006, Honolulu, Hawaii, October 2006, `http://www.phys.hawaii.edu/indico/contributionDisplay.py?contribId=454&amp;sessionId=186&amp;confId=3`.

[27] J. Kang, M. A. Luty and S. Nasri, arXiv:hep-ph/0611322.

[28] T. Moroi, arXiv:hep-ph/9503210.

[29] E. Brubaker *et al.* [Tevatron Electroweak Working Group], arXiv:hep-ex/0608032.

[30] S. J. J. Gates and O. Lebedev, Phys. Lett. B **477** (2000) 216 [arXiv:hep-ph/9912362].

[31] W. M. Yao *et al.* [Particle Data Group], J. Phys. G **33** (2006) 1.

[32] CDF Collaboration, `http://www-cdf.fnal.gov/physics/new/bottom/060921.blessed-sigmab/`.

[33] A. Arvanitaki, S. Dimopoulos, A. Pierce, S. Rajendran and J. G. Wacker, arXiv:hep-ph/0506242.

[34] T. Nunnemann, PoS **HEP2005** (2006) 320 [arXiv:hep-ex/0602039].

[35] E. Gallo, talk at ICHEP 2006, Moscow, August 2006, `http://ichep06.jinr.ru/reports/15_12p10_Gallo.pdf`.

[36] S. Chen *et al.* [CLEO Collaboration], Phys. Rev. Lett. **87** (2001) 251807 [arXiv:hep-ex/0108032]; P. Koppenburg *et al.* [Belle Collaboration], Phys. Rev. Lett. **93** (2004) 061803 [arXiv:hep-ex/0403004]. B. Aubert *et al.* [BaBar Collaboration], arXiv:hep-ex/0207076.

[37] M. Ciuchini, G. Degrassi, P. Gambino and G. F. Giudice, Nucl. Phys. B **527** (1998) 21 [arXiv:hep-ph/9710335]; Nucl. Phys. B **534** (1998) 3 [arXiv:hep-ph/9806308]; C. Degrassi, P. Gambino and G. F. Giudice, JHEP **0012** (2000) 009 [arXiv:hep-ph/0009337]; M. Carena, D. Garcia, U. Nierste and C. E. Wagner, Phys. Lett. B **499** (2001) 141 [arXiv:hep-ph/0010003]; P. Gambino and M. Misiak, Nucl. Phys. B **611** (2001) 338; D. A. Demir and K. A. Olive, Phys. Rev. D **65** (2002) 034007 [arXiv:hep-ph/0107329]; F. Borzumati, C. Greub and Y. Yamada, Phys. Rev. D **69** (2004) 055005 [arXiv:hep-ph/0311151]; T. Hurth, Rev. Mod. Phys. **75** (2003) 1159 [arXiv:hep-ph/0212304].

[38] LEP Higgs Working Group for Higgs boson searches, OPAL Collaboration, ALEPH Collaboration, DELPHI Collaboration and L3 Collaboration, Phys. Lett. B **565** (2003) 61 [arXiv:hep-ex/0306033]. *Search for neutral Higgs bosons at LEP*, paper submitted to ICHEP04, Beijing, LHWG-NOTE-2004-01, ALEPH-2004-008, DELPHI-2004-042, L3-NOTE-2820, OPAL-TN-744, `http://lephiggs.web.cern.ch/LEPHIGGS/papers/August2004_MSSM/index.html`.

[39] S. Heinemeyer, W. Hollik and G. Weiglein, *Comp. Phys. Comm.* **124** 2000 76, hep-ph/9812320; *Eur. Phys. J.* **C 9** (1999) 343, hep-ph/9812472. The codes are accessible via `www.feynhiggs.de` .

[40] H. E. Haber, R. Hempfling and A. H. Hoang, Z. Phys. C **75**, 539 (1997) [arXiv:hep-ph/9609331]; M. Carena, H. E. Haber, S. Heinemeyer, W. Hollik, C. E. M. Wagner and G. Weiglein, Nucl. Phys. B **580**, 29 (2000) [arXiv:hep-ph/0001002].

[41] J. R. Ellis, K. A. Olive and Y. Santoso, Phys. Lett. B **539** (2002) 107 [arXiv:hep-ph/0204192]; J. R. Ellis, T. Falk, K. A. Olive and Y. Santoso, Nucl. Phys. B **652** (2003) 259 [arXiv:hep-ph/0210205].

[42] H. Baer, A. Mustafayev, S. Profumo, A. Belyaev and X. Tata, JHEP **0507** (2005) 065 [arXiv:hep-ph/0504001].

[43] T. Jittoh, J. Sato, T. Shimomura and M. Yamanaka, Phys. Rev. D **73** (2006) 055009 [arXiv:hep-ph/0512197].

[44] K. Griest and D. Seckel, Phys. Rev. D **43** (1991) 3191.

[45] R. H. Cyburt, J. Ellis, B. D. Fields, K. A. Olive and V. C. Spanos, in preparation.